An environmental magnetic study of a marine sediment core from Disko Bugt, West Greenland: implications for ocean current variability

Jonas Andersson

Examensarbeten i Geologi vid
Lunds universitet - Kvartärgeologi, nr. 234
(15 hskp/ECTS)

Geologiska institutionen
Centrum för GeoBiosfärsvetenskap
Lunds universitet
2008

An environmental magnetic study of a marine sediment core from Disko Bugt, West Greenland: implications for ocean current variability

Master Thesis

Jonas Persson

Department of Geology
Lund University
2008

Contents

Cover Picture: The research vessel R/V Maria Sibylla Merian in Uummannaq Fjord during a scientific cruise to Disko Bugt. Courtesy of Ian Snowball.

An environmental magnetic study of a marine sediment core from Disko Bugt, West Greenland: implications for ocean current variability

JONAS PERSSON

Persson, J., 2008: An environmental magnetic study of a marine sediment core from Disko Bugt, West Greenland: implications for ocean current variability. *Examensarbeten i geologi vid Lunds universitet*, Nr. XXX, 35 pp. 30 points.

Abstract: An 11 m long marine sediment core was collected during a June-July 2007 scientific cruise with the German research vessel R/V Maria Sibylla Merian to the area of Disko Bugt, western Greenland. The core, designated 343340-6-1, was examined using environmental magnetic methods and X-ray fluorescence. The study contributes to a larger project designed to map the variability in sediment source and transport during the Holocene and relate these to ocean circulation, the behaviour of Greenland glaciers and climate change. Measurements of magnetic susceptibility and artificially applied magnetic remanences were performed on contiguous discrete samples from the whole length of the core. Complementary element analyses were done using X-ray fluorescence to detect shifts in major element content, which could be linked to changes in the magnetic record. The focus of the magnetic mineral identification was to distinguish between sections of elevated haematite and magnetite levels, as the relation between these two minerals is what primarily can be expected to cause any major shift in magnetic properties. An age-model was constructed for the core by means of correlation with another radiocarbon dated core from the same area, which indicates relatively ice-free conditions since approximately 8.5 kyr BP. The major mineral magnetic units comprise a relatively haematite-enriched section approximately covering the interval 1000-700 cm, followed by an area dominated by magnetite at ca. 700-400 cm. These two features comprise the main part of the core, from the bottom until around 350 cm depth, corresponding to an age of around 7.9 kyr BP. The uppermost part was not easy to interpret because the overall magnetic material content is diluted by organic content, which suggests that marine productivity increased after 7.9 kyr BP. It is argued that an increasing haematite component implies a stronger West Greenland Current (WGC). Parts that are instead dominated by magnetite, without signs of any significant amount of haematite, are thought to indicate a weaker WGC as the sediments would be influenced mainly by local, basaltic sources. These ocean current fluctuations may be connected to climate variations during the Holocene, but an improved age-model is needed to allow comparisons with other climate records.

Keywords: Disko Bugt, mineral magnetism, environmental magnetism, magnetic susceptibility, ARM, SIRM, IRM, HIRM.

Jonas Persson, Department of Geology, GeoBiosphere Science Centre, Lund University, Sölvegatan 12, SE-223 62 Lund, Sweden. E-mail: jonas.persson.987@student.lth.se

En miljömagnetisk studie av en marin sedimentborrkärna från Disko Bugt, västra Grönland: följder för havsströmmarnas variabilitet

JONAS PERSSON

Persson, J., 2008: En miljömagnetisk studie av en marin sedimentborrkärna från Disko Bugt, västra Grönland: följder för havsströmmarnas variabilitet. *Examensarbeten i geologi vid Lunds universitet*, Nr. XXX, 35 sid. 30 poäng.

Sammanfattning: Under en vetenskaplig expedition med det tyska forskningsfartyget R/V Maria Sibylla Merian till Disko Bugt, på västra Grönland, så provtogs under sommaren 2007 ett antal marina sedimentborrkärnor. Borrkärnan med beteckningen 343340-6-1 undersöktes inom ramarna för denna studie med miljömagnetiska metoder. Syftet med undersökningen har varit att kartlägga variationer i de mineralogiska egenskaperna över tid och utifrån det bestämma hur sedimentprovenansen har skiftat. Försök har dessutom gjorts att utifrån dessa slutsatser göra kopplingar till trender och förändringar i det regionala klimatet med betoning på variationer i havsströmmarna. Mätningar har gjorts med avseende på magnetisk remanens och olika magnetiska rest-egenskaper (ARM, SIRM, IRM). Genom att bestämma dessa parametrar så är det möjligt att spåra förekomsten av vissa magnetiska mineral. Eftersom ett sedimentprov består av en stor mängd individuella mineralkorn så kommer de erhållna värdena att representera de samlade magnetiska egenskaperna för samtliga korn i provet. Svårigheterna som därmed tillkommer har gjort att det bedömts som föga meningsfullt att sträva efter en fullständig beskrivning av det mineralogiska innehållet. Arbetet har koncentrerats på att undersöka fluktuationer i förhållandet mellan magnetit- och hematitberikade sediment, samt identifiera långsiktiga trender. Ytterligare analyser gjordes med röntgenflourosensce (XRF) för att studera förändringar i mängderna av olika grundämnen har också använts. Genom korrelering med en parallell borrkärna, som daterats med ett antal ^{14}C-analyser, har det kunnat fastsällas att den undersökta borrkärnan sannolikt inte är äldre än ca 8 500 år. Resultaten visar på ett betydande inslag av hematit i de äldre delarna, med ett skifte till mer magnetit-dominerade sediment vid en nivå av ca 750 cm, motsvarandes en ålder på omkring 8 000 år. En stadig nedgång i ett flertal magnetiska parametrar tar sin början vid ca 400 cm och övergår sedan i ett par kraftiga svängningar i de övre 200 cm. Denna nedgång har tolkats som början på Holocen, och förklaras med att det minerogena materialet spätts ut av en ökad biologisk produktion. Det argumenteras att hematitrika avsnitt av borrkärnan antyder en stark West Greenland Current (WGC), som är den norrgående ström som följer den grönländska västkusten. Delar av borrkärnan som saknar tecken på ett betydande hematitinnehåll, och som domineras av magnetit, antas signalera en försvagad WGC, då sedimenten här huvudsakligen tros vara dominerade av lokala, basaltiska källor. Dessa variationer i havsströmmarna, som indikeras av de undersökta magnetiska egenskaperna, kan eventuellt kopplas samman med klimatförändringar under Holocen. Det svaga underlaget för dateringen av borrkärnan medför att åldersbestämningen blir osäker, därmed är det i nuläget svårt att göra jämförelser med andra klimatarkiv.

.

Nyckelord: Disko Bugt, mineral magnetism, miljömagnetism, magnetisk mottaglighet, ARM, SIRM, IRM, HIRM.

Jonas Persson, Geologiska Institutionen, Centrum för GeoBiosfärsvetenskap, Lunds Universitet, Sölvegatan 12, 223 62 Lund, Sverige. E-post: jonas.persson.987@student.lth.se

”The ice was here, the ice was there,
the ice was all around,
It cracked and growled and roared and howled
Like noises in a swound!”

Rhyme of the Ancient Mariner,
Samuel Taylor Coleridge

1 Introduction

Scientific interest in the geographic and climatic conditions of Greenland was first pursued by Danish explorer Hinrich Johannes Rink. Rink mapped the area around Disko Bugt, and was the first to describe the inland ice sheet on Greenland, thus providing support for the emerging theories about past continental-scale glaciations in Europe (Weidecke & Bennike, 2007). Numerous studies have been conducted on the climate of Greenland, and it is believed that conditions in the remote arctic have fundamental significance for the climate in northern Europe.

As mentioned by Lloyd *et al*. (2005) and Lloyd *et al*. (2007) most palaeoclimatic studies in the investigation area have in the past been based on terrestrial and limnic material, and included such methods as geomorphological mapping of moraine complexes and construction of relative sea-level (RSL) curves. Investigations from shallow marine environments have been less frequent, but are now attracting a growing interest; particularly in the context of palaeoceanographic circulation studies.

The use of environmental magnetic methods as a means to study past climates is rapidly expanding (Evans & Heller, 2003). With a small number of relatively simple measurements it is possible to map the magnetic properties of a stratigraphic sequence in a core. Magnetic methods have been used in a few studies to examine the magnetic properties of sediment desposited close to ice-berg sources. This study has conducted magnetic analyses on marine sediments from Disko Bugt close to the Jakobshavn Isbrae, which is a major source of ice-bergs in the north Atlantic. Initial magnetic studies from the region have been published by Lloyd *et al*. (2005) and Lloyd *et al*. (2007) and these suggested that the method could be more widely used to complement other palaeoclimatic proxies.

The analysis methods used here include measurement of magnetic susceptibility, Anhysteretic Remanent Magnetisation (ARM), Isothermal Remanent Magnetisation (IRM) and Saturation Isothermal Remanent Magnetisation (SIRM), which are magnetic parameters routinely used in the field of environmental magnetism.The principle behind these methods is that the samples are exposed to a number of different magnetic fields and their response measured. Certain minerals are receptive to external magnetic fields, and will retain so called remanence. Magnetic remanence is acquired when electrons circling the atoms in the sample have been aligned according to a previously applied field, the sample has then been permanently magnetised. Magnetic minerals that are receptive to magnetisation include e.g. magnetite and haematite. Different minerals have unique magnetic properties and will respond in different ways. Sediment samples will be made up by numerous individual mineral grains, which determine the characteristics of the "mineral magnetic assemblage", The study here presented aims to outline the variability in sediment source in a marine core from Disko Bugt, central West Greenland. It is part of an international effort to "investigate the response of a major West Greenland ice stream during the Holocene". A relatively simple hypothesis is tested in this study: As ocean currents pass through the Vaigat strait north of Disko Island, they are enriched with haematite-rich material from the sedimentary bedrock areas along that coastline. At times of a weakened current regime in the bay, the haematite will not reach significant levels as to have any impact in the magnetic properties of the sediment deposited at the core location.

Using mineral magnetic methods, the occurrence of certain magnetic minerals at different levels of the core were examined. The shifts in sediment source were to provide hints to the variability in ocean currents and ice-sheet movements. The discharged ice or meltwater streams will carry with it sediment particles from the discharge area and from sources on their path. Presently the currents in the bay pass through an outlet north of Disko Island and then move south, passing to the west of the bay. The coring site of the examined sediment core is located in the western periphery of the Disko Bugt area, and can thus be expected to have received particles originating from the inner parts of the bay, via this route.

Due to the limited scope of this study the main focus of the mineral identification was to discern sediments with a haematite-signature from those that are more dominated by magnetite. The rationale behind this procedure is that the variability between these two magnetic minerals is expected to be the source of any major change in the magnetic parameters.

Based on the data obtained, and on the further treatment and interpretations made from it, large-scale trends in the sediment source variability could be identified. These trends have been connected to corresponding environmental events in the area.

2 Study area

Disko Bugt is located on the west coast of central Greenland (68˚30´N to 69˚15´N and 50˚00´W to 54˚00´W, Lloyd *et al.,* 2007) (see fig. 1). It is a marine embayment with a general depth of 200-400 m (Kuijpers *et al.,* 2001, Lloyd *et al.,* 2007). The northern half of the bay is dominated by Disko Island. The Egedesminde Dyb is a trough or valley, stretching some 100 km to the south-west, starting east of Arveprinsen Ejland. It was carved out of the seafloor by the stream of meltwater from the Jakobshavn Isbrae during the last glacial maximum, and has a deepest point of more than 900 m. (Long and Roberts, 2003; from Lloyd *et al.,* 2007). There are two major sources of ice-bergs in Disko Bugt, the Jakobshavn Isbrae and

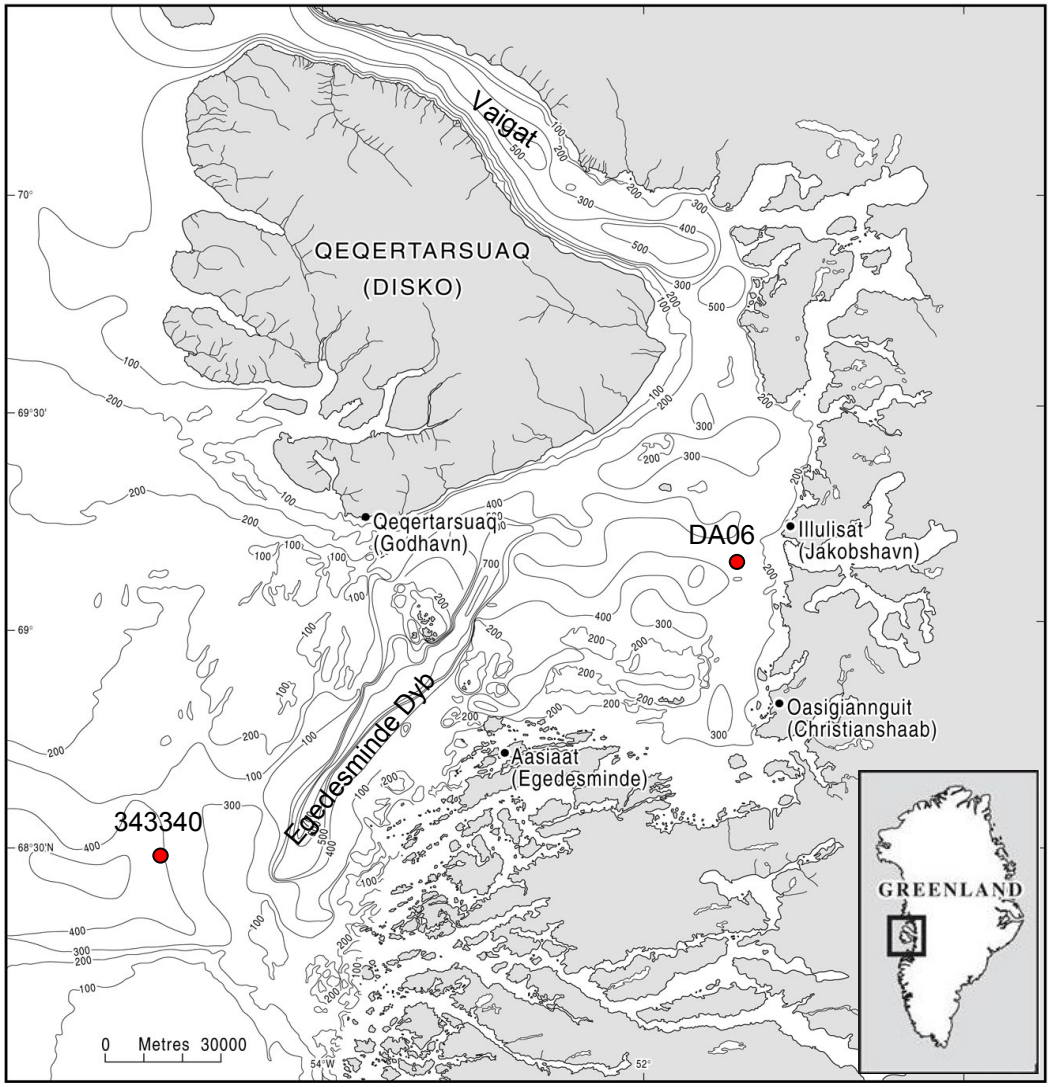

Fig. 1. Map depicting Disko Bugt with surroundings, and ocean floor depth. The coring site for the examined core 343340-6-1 is located to the lower left, in the outer parts of the Egedesminde Dyb submarine valley. Core DA06, used for correlation when esatablishing the age-model, is also marked on the map. (adapted from a version provided by J. Lloyd).

the Torsukattak ice-fjord in the northern part. The Jakobshavn Isbrae is today the fastest moving tidally controlled glacier in the world. It is situated 40 km east of the coastline at the edge of Jakobshavn Isfjord, just south of Ilulissat (Lloyd *et al.,* 2007). The discharge from the glacier is today 30-40 km^3/yr which corresponds to 1/3 of the total discharge from all of central west Greenland (Reeh, 1994; in Lloyd *et al.,* 2005). In addition it is also the "fastest calf-ice producing outlet" on Earth (26-36 km^3 annually) (Weidick *et al* 1990). Torsukattak is located 100 km north of Jakobshavn Isbrae, north-east of Arveprinsen Ejland Island. It is the recipient of a number of smaller surrounding ice-streams (Weidick & Bennike, 2007).

2.1 Geology

A basic outline of the local geological setting is shown in fig. 2. The ice-free hills of the mainland, east and south of Disko Bugt, consist of Precambrian gneiss belonging to the early Proterozoic orogenic belt. They generally reach no higher than 600 m asl. (Weidick *et al*., 1990). The Proterozoic bedrock along the coast consists of two main members. From Jakobshavn Isfjord stretching north, covering the southern half of Arveprinsen Ejland island, and reappearing in southeastern Nuussuaq is orthogneiss. The southern Rodeby domain is separated from the northern Niissuaq domain by the interrupting Atâ domain, which is composed of Archaean Atâ tonalite. This domain covers the northern half of Arveprinsen Ejland Island, and the area of the coast to the east of that island. The Atâ domain is host to a number of minor areas of supracrustal rocks, which are also present in minor spots along the

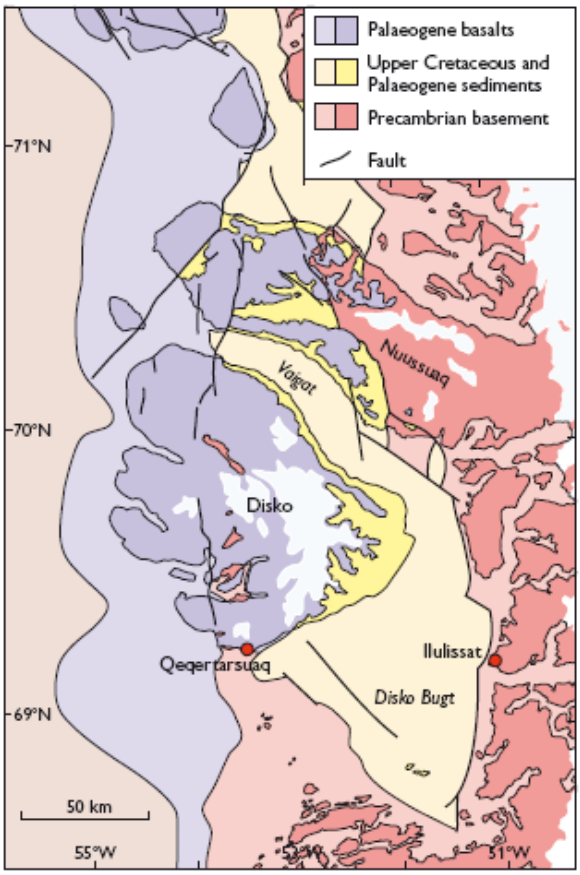

Fig. 2. A simplified overview of the distribution of bedrock types in the area around Disko Bugt. The eastern mainland is dominated by Precambrian gneiss, while Disko Island and the northwestern tip of Nuussuaq consist primarily of Palaeogene basalts. The east coast of Disko Island, as well as the mainland coast along the Vaigat strait consists of Cretaceous and Tertiary sedimentary bedrock. Adapted from Weidick & Bennike (2007), based on Chalmers *et al*. (1999) and Larsen & Pulvertaft (2000).

coast of Nuussuaq. These rocks consist mainly of greenstone, amphibolite, metagabbro and metasediments, and are concentrated to the Torsukattak area (Garde & Steenfelt, 1999).

On Disko Island and western Nuussuaq, Cretaceous and Palaeocene sedimentary rocks are preserved. Most of these deposits were covered by basalts during the Palaeocene and Eocene, but they are prominently represented along the southern coast of the Nuussuaq Peninsula, and on the east and north-eastern coast of Disko Island. Notably, this type of bedrock is present on both sides of the Vaigat strait (Weidick & Bennike, 2007). The sedimentary bedrock consists of both marine and lacustrine deposits from the Cretaceous, while the Tertiary deposits are exclusively marine (Birkelund, 1971). The eastern part of the sedimentary bedrock unit is dominated by fluvial sandstones. They are characterised by the presence of minor mudstones and coal. Further west, towards the western point of Nuussuaq Peninsula the deposits are

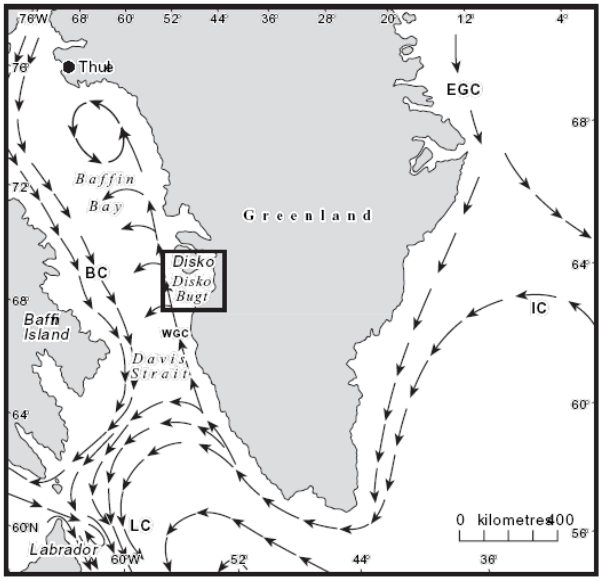

Fig. 3. Map showing the major ocean currents around Greenland (adapted from Lloyd *et al*., 2005). The East Greenland Current (EGC) which originates in the Arctic brings cold, low-saline waters, while the Irminger Current (IC) from the north Atlantic is warmer and has a higher salinity. These two are conjoined at the southern tip of Greenland and form the West Greenland Current (WGC).

dominated by mudstones. Extensive deposits of subbituminous coal have been exploited in the sedimentary bedrock of both on Disko Island and Nuussuaq (Henriksen *et al*., 2000).

The sedimentary bedrocks have been exposed to oxidation and are weathered. Thus, sediment dominated by material from these areas will probably contain relatively high amounts of well oxidised iron bearing magnetic minerals, such as haematite. Regarding the less weathered basalts that dominate most of Disko Island, and the sea-floor in the eastern parts of the bay, the major magnetic mineral is likely to be magnetite (Snowball, personal communication).

2.2 Oceanography

The present day oceanographic conditions around Greenland are illustrated in fig 3. The waters outside Disko Bugt are dominated by the West Greenland Current (WGC) which moves from the south. The WGC is produced by mergence of the East Greenland Current (EGC) and the Irminger Current (IC) at the southernmost tip of Greenland. The EGC originates in the Arctic and follows the whole stretch of the Greenland east coast. It is cold and has relatively low salinity. The Irminger Current originates in the North Atlantic and is thus warmer and has a higher salinity.

As the WGC moves north it is partly deflected to the west by the flux of cold melt-water from mainland Greenland. A strong branch south of

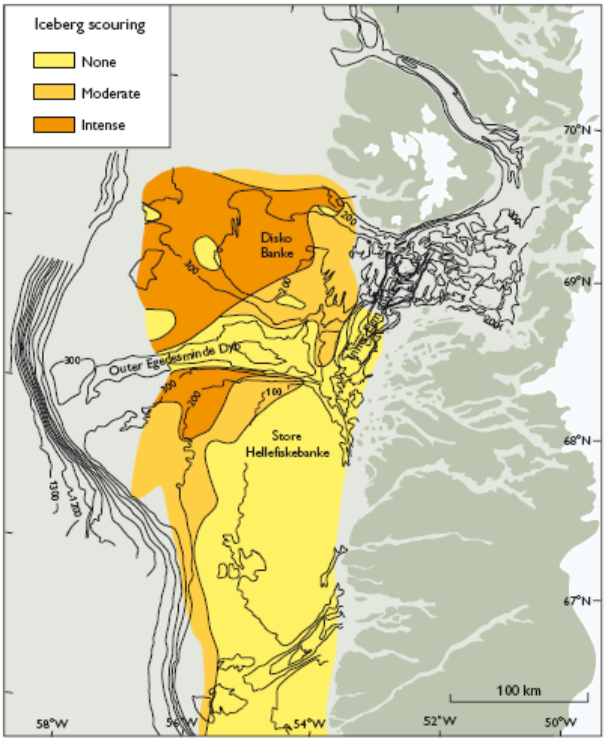

Fig. 4. Map showing iceberg scouring, indicating iceberg and material transportation routes during periods of glaciation in Disko Bugt (adapted from Brett & Zarudzki, 1979 in Weidick & Bennike, 2007).

Fig. 5. Map showing Disko Bugt and surroundings, with ages for ice-margin retreat adapted from Weidick & Bennike (2007), based on dates from Ingolfsson *et al.* (1990), Rasch (1997), Bennike *et al.* (1994), Bennike & Björck (2002), Long & Roberts (2003) and Long *et al.* (2006).

Labrador Current (LC). In Baffin Bay, to the north of Disko Bugt and south of Qaanaaq (Thule), the WGC is trapped by the LC and circles as a gyre. As the IC and the EGC meet there is initially poor mixing. The EGC component follows the shore closely, while the IC component takes a route further west and about 200 m below. The components of the WGC mix increasingly as they go further north, but are still distinguishable to the south of Disko Bugt (Lloyd, 2006).

In Disko Bugt the WGC is present as a deep, warm and saline water current. According to Buch (1981) in Lloyd *et al.* (2007) it is also detectable in the fjords on the east shore of the bay. On top of the relatively dense WGC is a layer of cold meltwater. The cold melt-water discharge and icebergs from Jakobshavn Isbrae are presently transported north, and pass through the narrow Vaigat strait north of Disko Island.

The north-bound WGC inside Disko Bugt brings calving ice bergs and melt-water from ice-streams through the Vaigat strait. Thus, as long as the WGC is strong enough and the ice-stream does not move to a more advanced position, icebergs will not be transported to the western parts of the bay. However, ice bergs and fresh water that escape the bay through the northern outlet will turn and travel south, and pass west of Disko Island. On their way south, many of them pass over the core site. These are the observed conditions of the recent past. When the ice-margin was much further west, access to the Vaigat outlet would be blocked, such that ice bergs and melt-water would then be directed westward. For example, markings on the sea floor from scraping ice-bergs show the directions of glacial discharge during the Last Glacial Maximum (LGM) (see fig. 4).

2.3 Climate change and reconstructions

The climate of Disko Bugt is presently low arctic maritime. The mean annual air temperature is –5.2° C, with a summer mean of 4.8° C (Lloyd *et al*., 2007). Palaeoclimatic records show that there have been dramatic and numerous shifts in the climatic conditions of West Greenland over the past 10 kyr.

The maximum extent of the inland ice sheet during the LGM occurred around 21 kyr BP but its spatial extend has not been determined in detail. It is likely that the whole of Disko Bugt was covered by the ice-sheet at the LGM. Around 14.7 kyr BP a period of warming conditions combined with with the effects of rising global sea levels caused recession of the ice margin (Weidick & Bennike, 2007).

The inland ice held a forward position on the outer coast of the bay until some 10 kyr BP. According to the deglaciation chronology for the Jakobshavn Isbrae ice-stream provided by Lloyd *et al.* (2005), Disko Bugt was deglaciated by 10.2 kyr BP. It is concluded that the ice margin by this time had retreated to a position in proximity to the eastern margins of the bay.

The early Holocene ice margin movements and climate variations around Disko Bugt were described by Long *et al.* (2006). Within the period known as the Holocene Thermal Maximum (HTM), which occurred over the first few thousand years of the Holocene, there was an interval of cooler conditions around 8.4-8.0 kyr BP. This is known as the GH-8.2 event and is detected in ice-core records from central Greenland (Long *et al*. (2006). This event brought a 5-7° C drop in mean annual air temperature over the centre of the ice sheet. Long *et al.* (2006) notes the apparent absence of ice-margin response to this cooling event in Disko Bugt. It is suggested the apparent lack of response to a major climate event could be because iceberg discharge at the time was dominated by calving, a process that is controlled mainly by local water depth and fjord topography, rather than by the regional climate. This is also supported by arguments given by (Warren & Hulton, 1990; Roberts & Long, 2005; in Long *et al*., 2006) that the lowland ice margin in Disko Bugt at the time of the GH-8.2 event was confined to a number of topographically restricted fjords.

The ice margin receded at c. 7.9 kyr BP and it passed its present day position around 6 kyr BP. Fig. 5 shows an ice-margin retreat chronology for the Disko Bugt area. Lloyd *et al*. (2007) mentions that the early Neoglacial cooling in West Greenland started around 5.0 to 4.2 kyr BP in Kangersuneq fjord in Disko Bugt and marked the end of the HTM.

Moros et al. (2004) present a detailed sequence of events regarding the Holocene climate history of the Disko Bugt area. Four major climate phases were identified. Initially there was the aforementioned HTM which lasted until 6.7 kyr BP according to their study. It was followed by a sudden decrease of surface layer temperatures in connection with a higher occurrence of ice rafting between 6.5 and 3.7 kyr BP. The age discrepancy between Lloyd *et al*.'s (2007) and Moros *et al*.'s (2004) definition of the end of the HTM is an example that demonstrates that the end of the HTM shows great temporal variability across Greenland and the north Atlantic. Between approximately 3.7 and 2 kyr BP, a transition to warmer and more unstable conditions took place. This interval of warmer climate is discussed by Weidick et al. (1990), where subsurface mapping and radiocarbon-dating of subfossils reveal warm and relatively ice-free conditions in the area around Jakobshavn Isfjord ca 4.7 to 2.7 kyr BP. Moros *et al*. (2004) further note that the ocean surface temperature then declined abruptly between 2 and 0.5 kyr BP. These fluctuations can also be traced in ocean current variability using foraminiferal records, as is shown by Lloyd *et al*. (2007).

3. Methods

The idea behind this study has been to record and interpret relevant magnetic data from the core labelled 343340-6-1. This data was processed in order to acquire knowledge about mineralogy and sediment source. A number of standard mineral magnetic methods were used, such as measurements of magnetic susceptibility, ARM, SIRM and IRM. The mineral magnetic data were calculated on a mass specific basis through dividing the value by the dry weight of the sample. This was done for all the subsample measurements: magnetic susceptibility and artificially induced remanence. The analytical work was performed at the Palaeomagnetic and Mineral Magnetic Laboratory (PMML) at the Department of Geology in Lund.

3.1 Sediment core recovery

The recovery of the gravity core 343340-6-1 was performed during the scientific cruise with the R/V Maria S. Merian in July 2007. The location of the core site is 68°23.834' 55°07.773, which is in the distal parts of Egedesminde Dyb underwater valley, at a depth of 461.3 m (see Appendix 1 for the core protocol). The core is 11 m long and was cut into in 11 segments of approximately 1m length immediately after recovery. Along with the parallel core 343340-5-1, the surface sediments were recovered with a multi-corer. A number of other adjacent sites were also cored over the duration of the cruise (see Dietrich *et al*., 2007 for the full cruise report). The core was marked and packed on the ship, and transported to Lund where it was stored in a cool room. The analytical work took place between January and March 2008. During the cruise a seismic profile for the coring station was constructed using an Atlas Parasound P70 subbottom profiling system (see Appendix 2 for the seismic profile of coring site 343340).

3.2 Core description

A lithological description of the retrieved core was done by means of ocular inspection. The colour terminology used in lithological descriptions in the cruise report (Dietrich *et al*., 2007) were adopted so as to achieve some degree of consistency and comparability.

3.3 Dating the core

One single radiocarbon dating was performed on foraminifera concentrated from the parallel core 343340-5-1 immediately after the cruise. Comparisons with the susceptibility curve from core DA00-06, described by Lloyd *et al.* (2005) and Kuijpers *et al.* (2001) were also conducted with the purpose of establishing an age-model for the core 343340-5-1. DA00-06 was retrieved from the area south of Disko Island, hence from a location somewhat further east than core 343340. By comparing features in the susceptibility diagrams, a correlation between the two could be made. An age-depth diagram was constructed from the provided values to evaluate the age model.

3.4 XRF

The upper 200 cm of core 343340-6-1 were analysed with XRF. The analysis was done with regard to 26 different elements, and was performed at the department of Geology and Geochemistry at Stockholm University using an Cox Analytical Itrax XRF core scanner with a step size of 5 mm. XRF data for the full parallel core 343340-5-1 was provided for nine elements onboard the R/V Maria S. Merian, comprising Al, Si, S, Cl, K, Ca, Ti, Mn and Fe. The equipment used was an Avaatech XRF Core Scanner, set with a resolution of 1 cm. The data from both XRF scanners are provided in counts per second (cps) and are not adjusted for sediment density.

3.5 Subsampling for mineral magnetic analysis

Each one-meter core section was split longitudinally, using an electrical circular saw to cut through the plastic core liner. A copper wire was used to split the sediment core. One working half of each section was used for the analyses, while the other archive half was packed and placed in storage at 4^{o} C. The core used for sub-sampling was cleaned using plastic scrapers to get an undisturbed surface. The sections were sub-sampled for mineral magnetic analysis using standard 2.2x2.2x2.2 cm plastic sample cubes weighing 4.34g, with an internal volume of 7 cm^{3}. The cubes had small holes drilled to the bottom in order to let the air escape when the container was pressed down into the sediment of the core. Samples were taken continuously, with an interval of approximately 2.25 cm, along the entirety of the core sections. The samples were also weighed on a balance in a wet state and once more after drying at 40^{o} C, after the magnetic susceptibility and remanence measurements were completed.

3.6 Magnetic susceptibility

Magnetic susceptibility is described by Butler (1992) as "*the ease with which a material changes its magnetic field under the influence of a magnetic field*".

The low field surface magnetic susceptibility of the core sections was measured using a Tamiscan TS-1 automatic logging conveyor (see fig. 20 in Appendix 4). This automated scanning system is equipped with a

Bartington MS2E1 surface scanning sensor coupled to a Bartington MS2 meter. It was set to measure the susceptibility every 5 mm over the length of each core section using the 1.0 sensitivity scale. The split halves of core 343340-5-1 had been measured with the same equipment, using the same settings, onboard the R/V Maria S. Merian during the scientific cruise.

Each subsample was then measured manually for low field magnetic susceptibility using a Geofyzica Brno KLY2 Kappabridge (See fig. 21 in Appendix 4). The property measured by the Kappabridge device is the ratio of induced magnetisation (M) to imposed magnetic field (H). This parameter, known as bulk susceptibility, is abbreviated as κ and is a dimensionless ratio with the output from the Bartington MS2 meter in 10^{-5} SI (System Internationale). When corrected for dry density the units are given as magnetic susceptibility (χ) in m^3kg^{-1}.

3.7 Remanent magnetisation measurements

Anhysteretic Remanent Magnetisation (ARM) is a common method in mineral magnetic studies, as well as in the magnetic recording industry. It applies a relatively strong alternating field (AF) with gradually reduced amplitude, but to generate an ARM in the samples a small stable direct biasing field is superimposed on the AF. The induced ARM will have a well-defined direction. The acquisition of the ARM depends on the response time of the minerals in the sediment which carries the remanence (Snowball, 1999). The ARM was induced in the samples using an Enterprises model 615 anhysteretic remanent magnetiser (See fig. 22 in Appendix 4), with a maximum AF strength of 100 milliTesla (mT) and a bias field of 0.1 mT.

During Saturation Isothermal Remanent Magnetisation (SIRM), the sample is exposed to a strong magnetic field at a steady (room) temperature so as to achieve magnetic saturation. Thompson & Oldfield (1982) describes SIRM as a tool mainly for measuring the content of magnetite in a sample. It is, however, also dependent on grain size and the presence of other magnetic minerals. Other magnetic minerals, such as hematite are also known to produce a strong remanent magnetization (albeit much weaker than for magnetite). The SIRM was applied using a Redcliffe 700 BSM pulse magnetiser with a field strength of 1 Tesla (T) (See fig. 23 in Appendix 4). The pulse magnetiser functions by building a charge of correct size in a system of electric capacitors, which is released during a few milliseconds.

In this study two backfield Isothermal Remanent Magnetisations (IRMs) were induced to determine the coercivity characteristics of the samples. IRM was applied in two series, with field strengths of –100 mT and –300 mT. The application of the –100 mT field was performed using a Molspin pulse magnetiser (See fig. 24 in Appendix 4). The charge is released and the magnetic field is applied as a short pulse (Walden, 1999). The –300 mT field was induced with a Redcliffe 700 BSM pulse magnetiser.

The acquired ARMs, SIRMs and backfield IRM's were measured with a Molspin "minispin" magnetometer (See fig. 25 in Appendix 4) which was calibrated using a standard with a nominal value of 964 $10^{-3}Am^{-1}$. Correction for dry density and the assumed volume of the standard permits the calculation of mass specific units in Am^2kg^{-1}.

Table 1. Typical magnetic properties and ratios for some natural minerals and rock types. Compiled from Maher *et al* (1999) and Thompson & Oldfield (1986).

Substance	**χ (10^{-6} m^3 kg^{-1})**	**ARM (mA m^2 kg^{-1})**	**SIRM (Am^2 kg^{-1})**	**SIRM/χ (kA m^{-1})**	**S_{-100}**	**ARM/ SIRM**	**ARM/χ (kA m^{-1})**
Magnetite (soft)	560	18	9	1,6	0,97	0,02	0,03
Magnetite (hard)	400	110	22	55	0,85	0,005	0,3
Titanomagnetite (soft)	170	80	7	10	0,82	0,004	0,5
Titanomagnetite (hard)	200	480	12	60	0,34	0,04	2,4
Haematite	0,6	0,002	0,24	400	0,003	0,001	0,01
Ilmenohaematite	25	480	8	320	0,13	0,004	19
Iron	2000	800	80	40	0,8	0,01	0,4
Basalt	1,8		70	40	0,8		
Sandstone	0,1		0,5	7	0,8		
Gneiss	0,05		7,5	150	0,7		

3.8 Data treatment

S-ratios were given by dividing each IRM value with corresponding value from the SIRM (S_{-100}= IRM_{-100mT}/SIRM and S_{-300}=IRM_{-300mT}/SIRM). The S-ratios can be used to determine the relative contribution of haematite versus magnetite, or "hard" antiferromagnetics and "soft" ferrimagnetics (Oldfield, 1999; Maher et al., 1999 and Evans & Heller, 2003).

The High Field Isothermal Remanent Magnetisation (HIRM) is the isothermal remanence acquired below a certain field (in this case -100 and -300 mT). It is calculated according to [(1 + S-ratio)*(SIRM/2)] respectively (after Snowball, 1993). According to Thompson & Oldfield (1986) HIRM can show contributions from imperfect ferrimagnets (canted antiferromagnets) such as haematite and goethite. It is a useful tool to distinguish contributions of relatively hard magnetic minerals such as haematite and goethite. The S-ratio calculated at -300 mT is preferred if the aim is to detect canted antiferrimagnetics because the ratio at -100 mT can be influenced by changes in magnetite grain size.

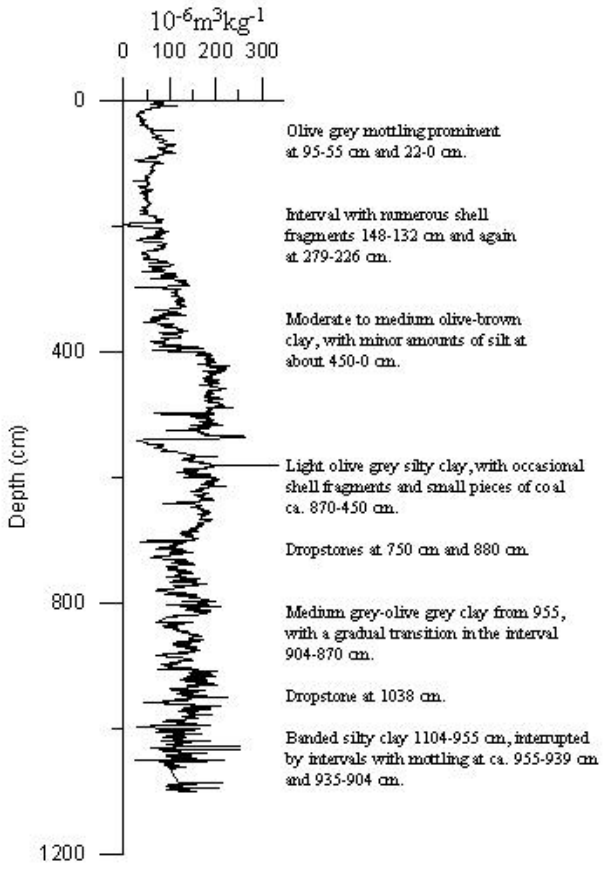

Fig. 6. An overview of the lithology the core, with the curve for magnetic susceptibility included for comparison. A full lithological discription is found in Appendix 1.

The calculated ratios ARM/SIRM and ARM/χ can show magnetic grain size variations for ferrimagnetic minerals (such as magnetite). Finer particles will then reveal a higher value for these ratios (Maher & Thompson, 1999 and Evans & Heller, 2003). SIRM/χ, χ_{ARM}/χ and χ_{ARM}/SIRM are other typical interparametric ratios used routinely in environmental magnetic studies.

4 Results

The results from the various measurements and calculated ratios show several distinct intervals in the core. The characteristics of each interval can be traced in multiple parameters, and the major trends appear to be relatively clear.

4.1 Lithological description

Appendix 3 contains the full lithological description of core 343340-6-1, while fig. 6 presents a summary. Silty clay dominates the core, with an increasing organic content towards the top, as indicated by the gradually darker colour seen especially in the upper 400 cm. The presence of mottling has been identified in the core sections between 1004 and 904 cm, and from 101 cm to the top of the core. Dropstones have been noted exclusively in the lower 400 cm, while shells (mostly bivalves) have only been observed above 700 cm.

4.2 Magnetic susceptibility

The results from the long core magnetic susceptibility measurements, using the Tamiscan TS-1 system, are displayed in fig. 8. The values are comparable to the results obtained from the onboard analysis of the parallel core 343340-5-1. The values range between 25 and 350 10^{-5} SI. Although many of the individual peaks and dips differ between the two, these can be explained by the presence of dropstones, shells on or just under the surface of (and possibly below) the cores. Undulations on the core surface can also produce apparent changes that do not reflect the properties of the sediment. Thus, the most extreme peaks and dips have therefore been removed from the curve for increased clarity.

The scanning magnetic susceptibility curves from the two cores show the same variability below a depth of 150 cm and these sections of the two cores are can be considered comparable to each other regarding magnetic properties. However, the two scanning MS profiles are distinctly different above 150 cm.

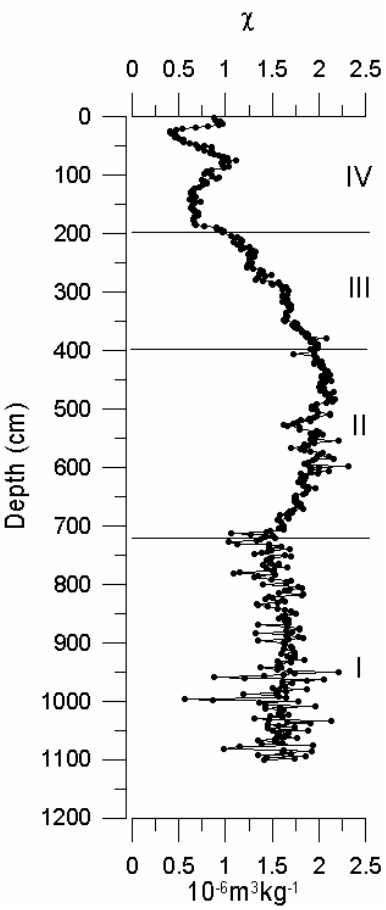

Fig. 7. Mass specific magnetic susceptibility (χ). The curve has been divided into four zones based on its general characteristics. Zone I in the bottom of the core, has some large initial fluctuations which are possibly due to ice-rafted debris (IRD). Zone II is characterised by a plateau of elevated values. Zone III shows a stable and steep downturn in susceptibility. Zone IV, which contains the upper 200 cm of the core, displays some dramatic peaks and troughs.

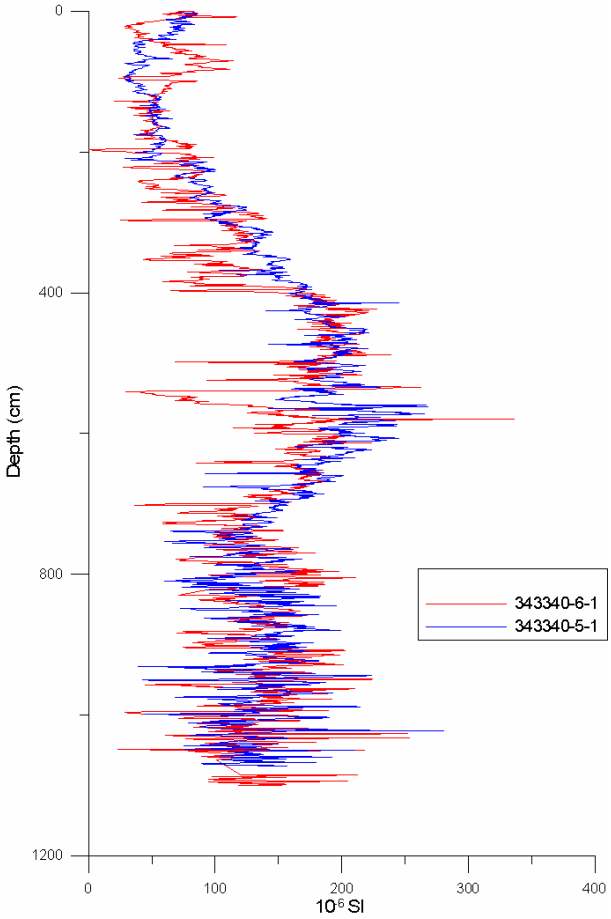

Fig. 8. Diagram comparing the long core magnetic susceptibility curves for the two parallel cores 343340-5-1 and 343340-6-1. Core 343340-5-1 was measured onboard the ship during the 2007 scientific cruise when the cores were recovered. Core 343340-6-1 was measured in the palaeomagnetic laboratory at the Geobiosphere Center, Lund University. Both measurements were performed using a Tamiscan TS-1 automatic conveyor system equipped with a Bartington MS2E sensor.

Mass specific magnetic susceptibility (χ) ranges between 0.5 and 2.25 $10^{-5}m^3kg^{-1}$. Based on the characteristics of the χ curve the core has been divided into four mineral magnetic zones as seen in fig. 7. In the lower parts of the core (Zone I - 1104 cm to 700 cm), the curve indicates relatively high amplitude fluctuations in magnetic mineral content. There is a slight general trend of decreasing magnetic susceptibility and the amplitude of the fluctuations become less pronounced towards the top of this section. In Zone II (700 cm to 470 cm) there is an initial steep rise in magnetic susceptibility towards maximum values at a depth of 500cm. At approximately 470 cm the c starts to fall. Zone III (400 cm to 190 cm) outlines the decline following the plateau in Zone II. The decline is smooth, and only minor small-scale fluctuations are visible. A section of stable magnetic susceptibility marks the start of Zone IV at 190 cm. The curve then levels out and a period of temporary stability is reached. It then climbs to a large peak, followed by a distinct trough. The uppermost part shows a fast and steep recovery at about 13 cm. It should be noted that the top of the core most likely does not contain the sediment-water interface.

4.3 Magnetic remanence

Zone I (1104-725 cm). In accordance with the χ data the ARM and SIRM data also indicate high-frequency and high amplitude fluctuations in magnetic mineral concentration in Zone I. SIRM values reach 25 $10^{-3}Am^2/kg$ in this zone. The S_{-100} ratio varies around -0.8 and the $HIRM_{100}$ values reach a maximum of 3 $10^{-3}Am^2/kg$. The SIRM/χ ratio varies between 8 and 14 10^3Am^{-1}, while the χ_{ARM}/χ ratio peaks at 2 in this zone. HIRM300 values are low at less than 0.4 $10^{-3}Am^2/kg$.

Interpretation: The low S_{-100} ratio and SIRM/χ values show that the magnetic properties of Zone I are dominated by a soft ferrimagnetic, most likely titanomagnetite. The concentration of this magnetic mineral is quite variable in this zone and probably reflects the heterogeneous distribution of coarse grained ice-rafted debris (IRD) and laminations that are described in the lithostratigraphy. The discrepancy between the SIRM/χ and magnetic susceptibility is interpreted as enhanced levels of haematite, especially in the upper parts of this zone.

Zone II (725-400 cm). After an initial rise in magnetic susceptibility, values stabilize around 1.8-2.2 $10^{-5}m^3kg^{-1}$and forms a plateau interrupted only by occasional peaks and dips in the lower half of the zone. ARM and SIRM data shows a greater degree of variability and fluctuations, and both reach their peak values in this zone, for ARM this is at 481 cm and for SIRM at 483.5 cm. The S_{-100} ratio remains around -0.8, while HIRM100 displays less variability. The SIRM/c curve falls sharply, forming a trough with several minor peaks within. At the top of the zone it reaches a peak at 485 cm. Values for $HIRM_{300}$ remain relatively stable, with a baseline below 0.4 $10^{-3}Am^2/kg$. The curve also peaks distinctly at 513.5 cm.

Interpretation: The presence of a magnetic susceptibility plateau and the values of SIRM/χ indicate enhanced levels of magnetite in this zone.

Zone III (400-200 cm). A fall in magnetic susceptibility is also reflected by declining trends in ARM and SIRM values. ARM data stabilize below 0.1 10^{-3} Am^2/kg, while SIRM drops to around 5 10^2 Am^2/kg. S_{100} values show a slight increase throughout this zone, while the $HIRM_{100}$ curve declines moderately. $HIRM_{300}$ is stable, with a minor rise.

Interpretation: This zone represents a transition to significantly lower levels of magnetic material, as shown by the fall in magnetic properties. It is further reflected by the gradual transition to a darker colour with a higher ratio of organic material, as seen in the lithological description.

Zone IV (200-0 cm). χ data displays some large-scale fluctuations in this zone. Values level out initially, but then starts to climb sharply until a peak is reached. This peak is followed by a sharp dip after which another steep rise begins. Corresponding patterns are not seen in the ARM or SIRM curves, which remain relatively stable. The S_{-100} ratio rises to a plateau, which is followed by two distinct peaks. The uppermost of these peaks contains the highest values of this curve, at just below -0.5. These peaks are also reflected in the SIRM/c and c_{ARM}/c which both have a single peak, which covers the interval of peaks in the S_{-100} diagram. Furthermore, both the $HIRM_{100}$ and $HIRM_{300}$ displays double peaks in this section.

Interpretation: The sudden shifts in magnetic susceptibility in this zone are not reflected in any other parameter. There are however two spikes in values, as seen in the S_{-100}-ratio, SIRM/χ, χ_{ARM}/χ and both the HIRM parameters. These could be interpreted as a presence of haematite, although it is an uncertain conclusion. The relatively low levels of magnetic material in the upper parts of the core could make the data sensitive to interference, giving rise to misleading patterns.

Some trends can be clearly seen in the diagrams in fig. 10. All concentration parameters and ratios that include magnetic susceptibility as the normaliser, (with the exception of $HIRM_{300}$) show high amplitude variability between the bottom of the core and 400 cm. Zone II displays some degree of stability in the short-term fluctuations, while there is also a prominent peak or plateau. The curves then tend to decline rapidly and reach somewhat stable values. However, several curves also show sudden large peaks and dips in the uppermost section.

The ARM diagram (fig. 10b) displays a curve distinguished by large and numerous fluctuations. Several overlying trends can be noted. Large, higher-frequency fluctuations that occur from the bottom and

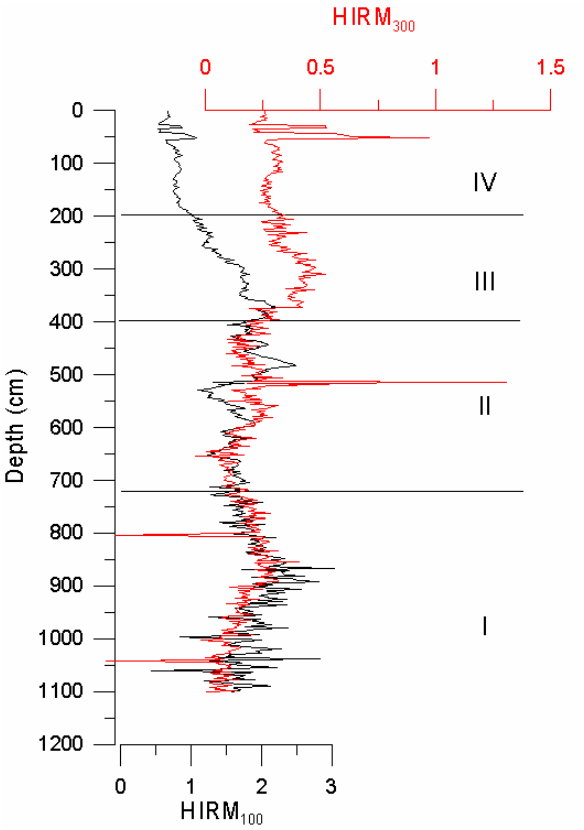

Fig. 9. Diagrams showing the deviations between the two HIRM parameters. These are used to distinguish "hard" antiferrimagnetics (such as haematite) in the sample. The difference between the two shows that not all the magnetite present was saturated at –100 mT backfield. Peaks in this curve can thus be due to areas of sorted magnetite, whereas the HIRM300 will not be grain size dependant. Note that different scales have been used for the two curves in this figure.

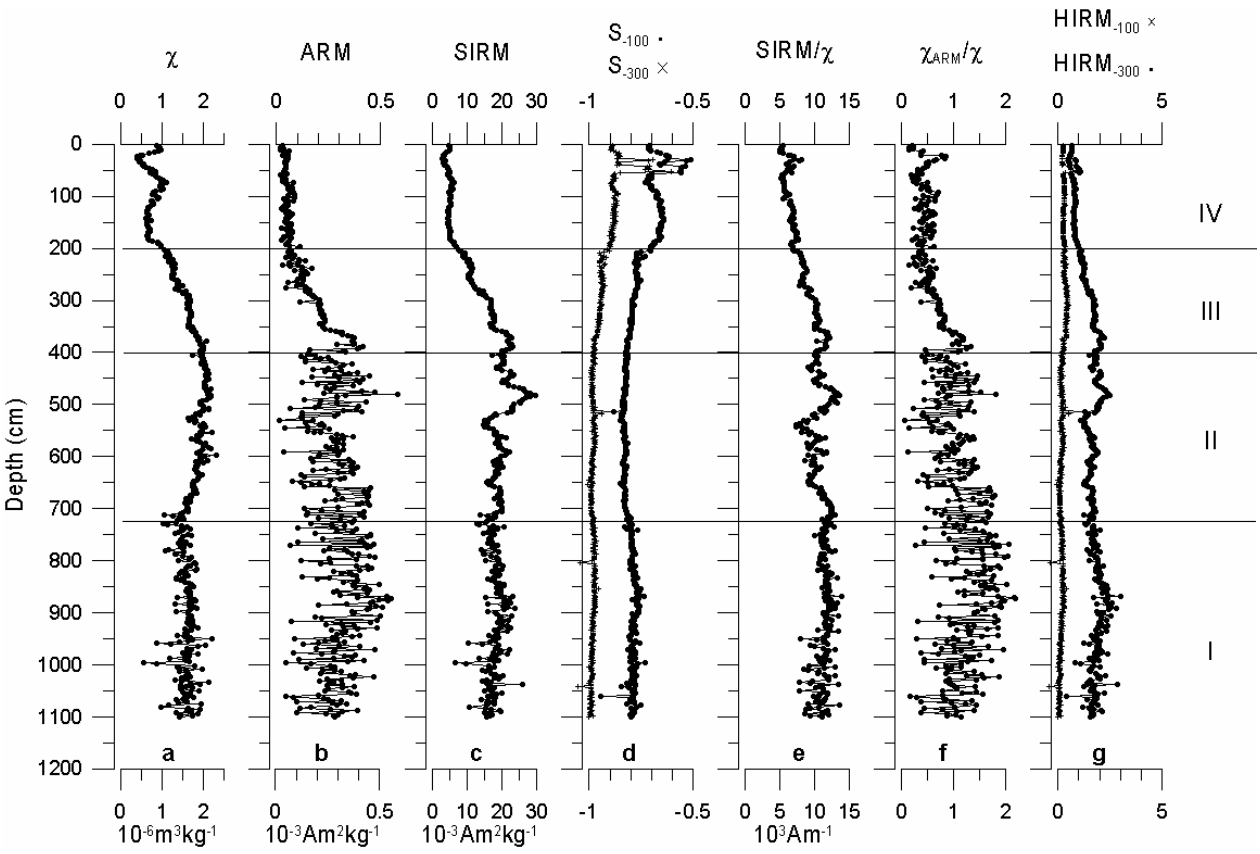

Fig. 10. Diagrams illustrating the results from measurements of magnetic remanence as well as a number of parameters calculated from measured values. The curve for magnetic susceptibility has been included for comparison. All diagrams are based on values in mass specific units (10^{-6} m^3/kg). a: Magnetic susceptibility; b: Anhysteretic Remanence Magnetisation (ARM) c: Saturation Isothermal Remanence Magnetisation (SIRM); d: S-ratios, calculated from IRM_{100mT}/SIRM; e: SIRM/χ; f: χ_{ARM}/χ; g: $HIRM_{100}$ and $HIRM_{300}$. χ, ARM and SIRM were measured on 481 discrete subsamples covering the entire length (1104 cm) of core 343340-6-1.

until ca 400 cm are superimposed on lower frequency variability. These are especially clear at levels 700-530 cm, but can be traced both up and downwards from this area. From the bottom values climb to reach a major peak at 875 cm, only to fall back again thereafter. A major turnover takes place at around 350 cm. After a steep and steady decline, values appear to be levelling out and reach a stable baseline around approximately 0.05 Am^2/kg. Small-scale, regular fluctuations continue until the top, but are much less pronounced.

The reoccurring pattern of variations in Zone I is further shown in the SIRM diagram (fig. 10c). While values for magnetic susceptibility appear to fall throughout this zone, the SIRM display a slight increase. In the middle section of Zone I there is a distinct rise, after which the curve falls back. Zone II further deviates from the susceptibility trend by the lack of a clear plateau. There are a few minor areas which have elevated values, and also one large peak. Above the peak, a level of higher values is sustained, but in Zone III they enter a steep decline. Zone IV is relatively stable, the only visible feature being a small trough towards the top.

The S_{100}-ratio diagram (fig. 10d) shows some initial fluctuations, although the variability is moderate. The large-scale trend is that there is a major trough stretching over about 700-400 cm. Here values go well below –0.8. Beyond the trough there is a sudden climb to a stable plateau with sustained values at around -0.73. After the end of the plateau, there is at first a dip and then two large peaks with another dip in between. The highest value of this curve is found in the latter of these peaks, reaching –0.51. The diagram ends with a dip in the uppermost part of the curve.

$HIRM_{100}$ and $HIRM_{300}$ show a great deal of deviation (as seen in their curves in fig. 9 and fig. 10g). The $HIRM_{100}$ has in Zone I, apart from the fluctuations seen in the other diagrams, also a large and in the long-term relatively stable peak. Zone II is characterised by large changes but less short-term fluctuations, with two dips at about 650 and 540 cm depth. These are followed by a significant peak just above 500 cm. In the upper part of Zone II values remain at a generally high level, although there is a trough followed by another peak. The curve levels out as it reaches Zone III, where values decline at a stable rate. The major features of Zone IV are the two sharp peaks in the uppermost part of the core. $HIRM_{300}$ displays a

regular pattern of higher and lower values throughout the curve. There are three major areas of elevated values at 850, 560 and 310 cm. At 513 cm there is a large, but short-lived peak, reaching maximum values for the curve. The two final peaks shown in the $HIRM_{100}$ diagram is also reflected in the $HIRM_{300}$ curve, at 52 and 30 cm. The general trend in the $HIRM_{300}$ diagram is that there is a slight increase in values towards the top.

4.4 Magnetic ratios

Comparisons between the SIRM/χ curve and magnetic susceptibility point towards a common trend (fig. 11). In Zone I, between about 925-700 cm the susceptibility curve as well as the SIRM/χ diagrams show a similar decline. However most of the SIRM/χ values are still higher in this interval than further down in the core, while the susceptibility values reach down below the imagined baseline of the lower parts of the curve. Again, in Zone II, where the plateau of elevated susceptibility is located, there is a distinct decline in the SIRM/χ. The two peaks in the SIRM/χ, which are rising above this large trough appears to coincide with the two sharp dips on the plateau of the magnetic susceptibility curve. Zone III shows a steady decline in overall magnetic content, which is reflected in both diagrams. While Zone IV starts with a sharp drop in susceptibility, the SIRM/χ remains almost unaffected. The final large dip in susceptibility is again mirrored by the SIRM/χ, as a strong peak is seen at the very same level.

The dependence on sorting in the mineral magnetic record was examined by comparing the two grain-size dependant parameters SIRM/χ and χ_{ARM}/SIRM, as presented in fig. 12. The foremost result gained from this comparison is that the major peak at about 500 cm, appears to be related to grain-size properties rather than mineralogy.

Inter-parametric plots (fig. 13, 14 and 15) show a division between two major groups of values, assumingly representing distinct mineral magnetic conglomerates. The lowermost of these groups appears to correspond roughly to Zone I and II, while the second group represents the two upper zones (IV and V). In the plot between the two S-ratios (fig. 15), Zones I and II can also be distinguished in different clusters.

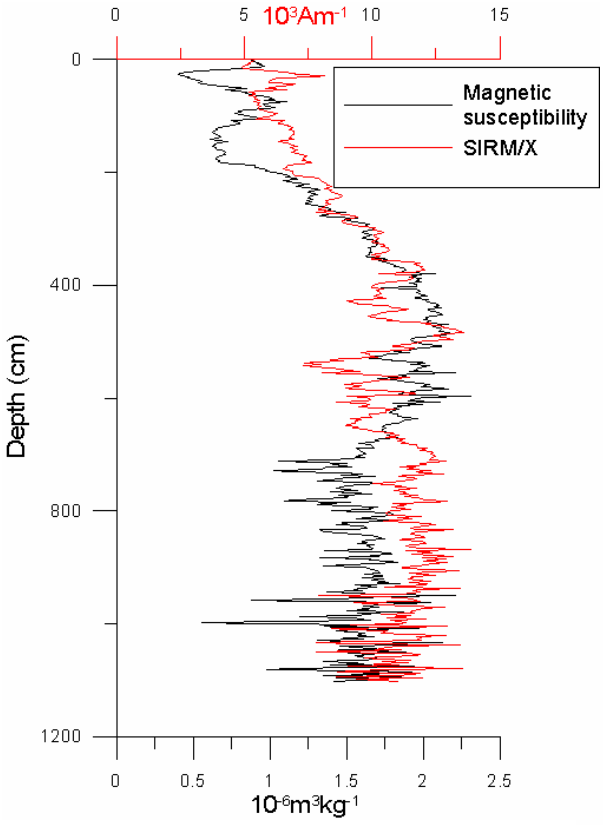

Fig. 11. Comparison between the curves for magnetic susceptibility (χ) and the ratio SIRM/χ. The divergence between the two is used to identify areas of excess haematite. Parts where the SIRM/χ curve is higher than the χ, is interpreted as a haematite-signature.

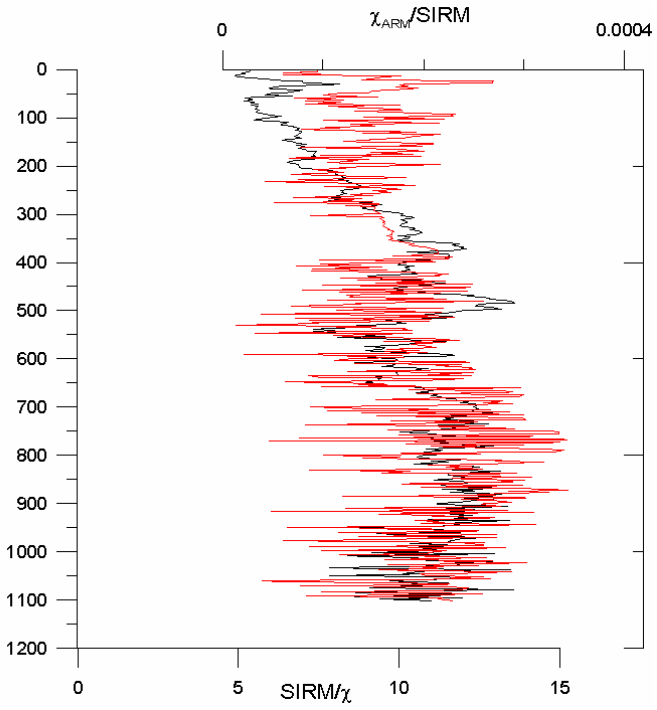

Fig. 12. Comparison between the two grain size dependant parameters SIRM/χ and χ_{ARM}/SIRM. Elevated values for these parameters indicate finer magnetic grain sizes, which may be an effect from sorting of the sediment.

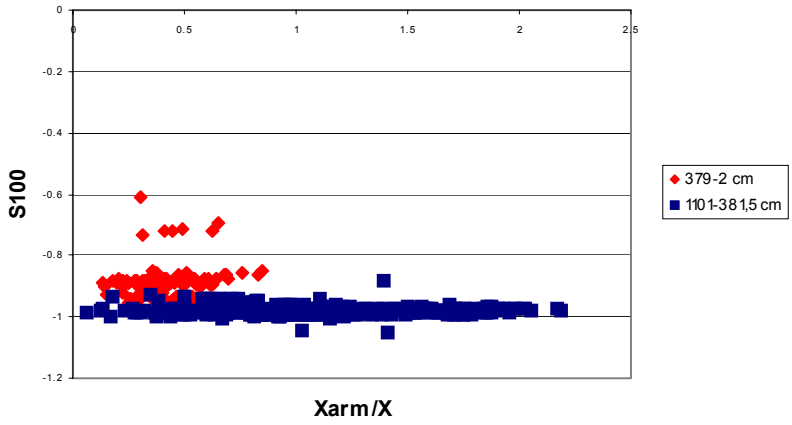

Fig. 13. Biplot between the S_{100}-ratio and χ_{ARM}/χ. Two groups of values are visible in the intervals 1104-381,5 cm, representing Zones I and II, and 379-2 cm showing Zones III and IV.

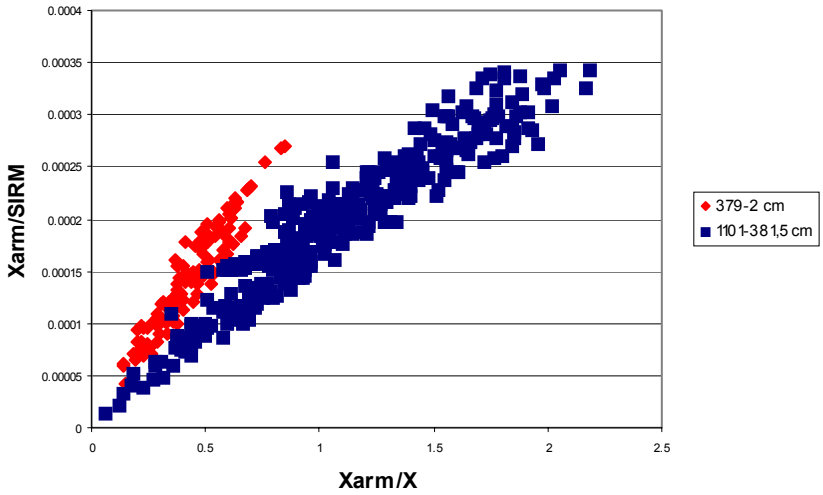

Fig. 14. Biplot between the χ_{ARM}/SIRM and χ_{ARM}/χ. Data points from mainly the upper two zones are grouped in a distinctly deviating direction compared to the bulk of the values.

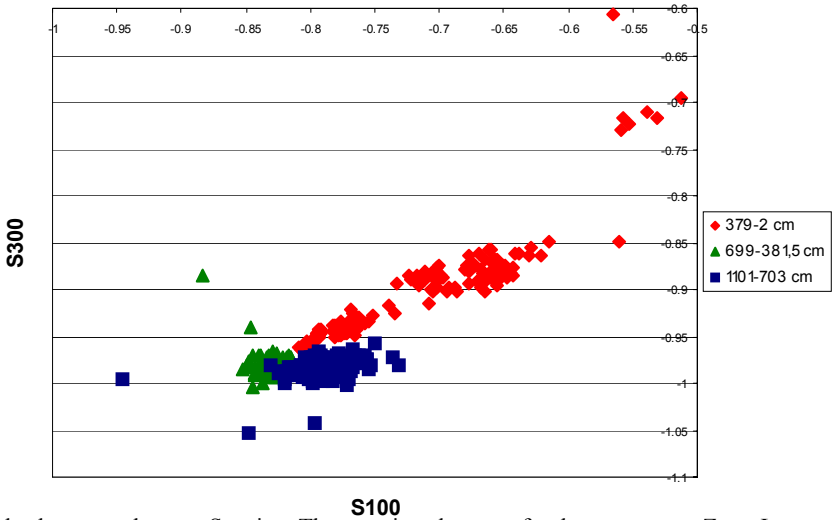

Fig. 15. Biplot between the two S-ratios. Three major clusters of values are seen. Zone I correspond to the lower, middle group, while Zone II is represented by the lower left group. Zones III and IV appear share the uppermost cluster in the diagram.

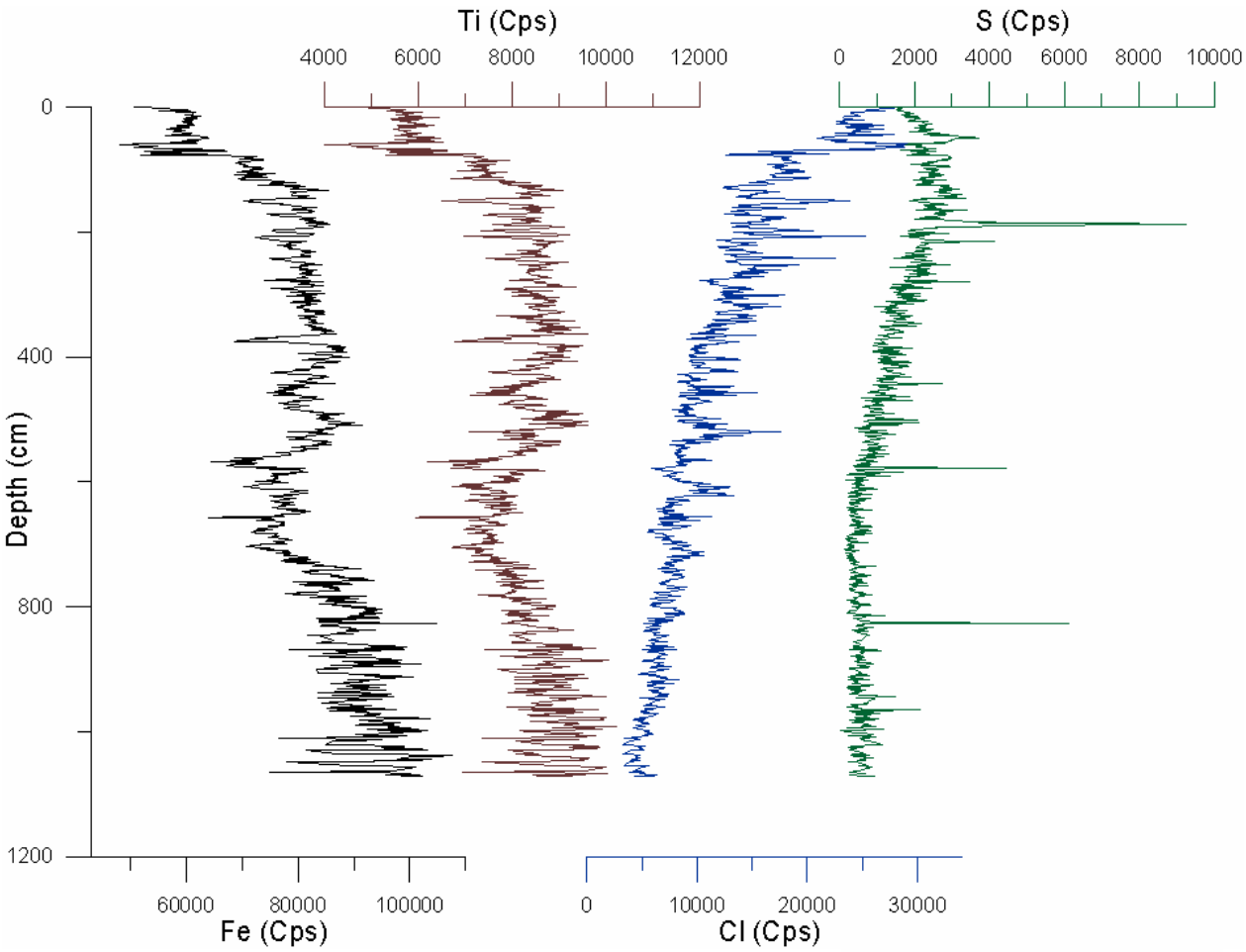

Fig. 16. Diagrams showing the results of XRF analysis for the elements chlorine, iron, titanium and sulphur, on gravity core 343340-5-1, a parallel core extracted from the same site as core 343340-6-1. Two distinct trends can be distinguished. Levels of iron and titanium are declining, to end in a steep fall. Sulphur and chlorine on the other hand, are both climbing. The increase in chlorine also appears to be accelerating towards the top.

4.4 XRF

The full results from XRF analysis on core 343340-6-1 are given in Appendix 5. A few notable trends can be observed from the results of the XRF scans. As core 343340-6-1 was only scanned for the upper 200 cm, data from core 343340-5-1, provided by Snowball via personal communication, will mainly be used for the interpretations.

The elements presented in fig. 16 and 17 are those which are deemed to be of interest for this study. Sulphur and titanium show opposite trends throughout the core. The long-term patterns indicate a fall in titanium and a rise in sulphur. The iron levels follow the same path as the titanium curve. The curves from the analysis performed on core 343340-6-1 also show a slight drop in titanium, while sulphur remains approximately stable.

The chlorine levels, reflecting the salinity of the sea water and which may be of some interest, can also

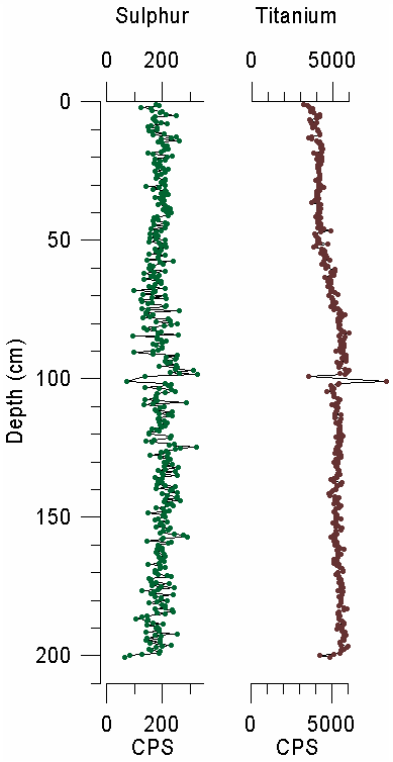

Fig. 17. Diagrams showing the results of XRF analysis for the elements titanium and sulphur on the upper 200 cm of gravity core 343340-6-1. The only change that can be clearly seen is the continuous drop in titanium.

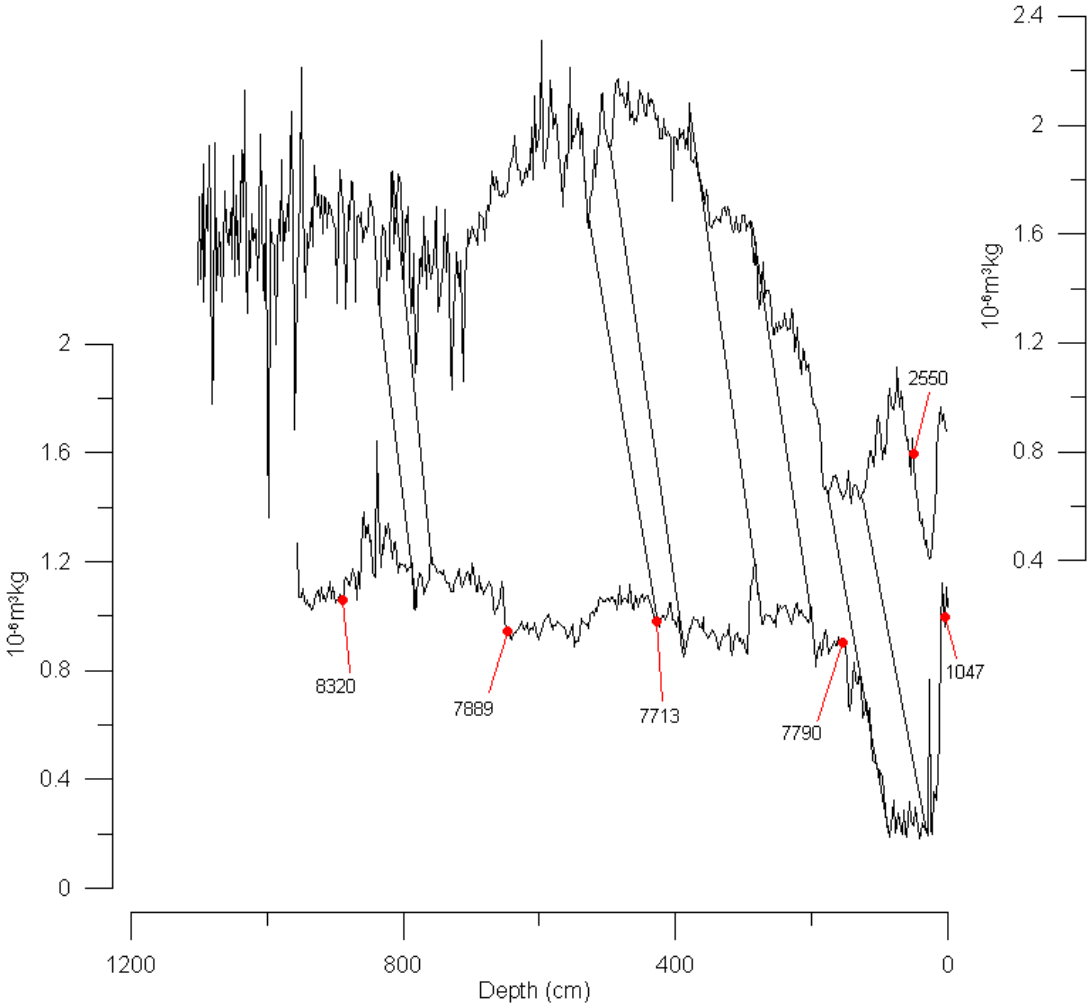

Fig. 18. Correlation between the magnetic susceptibility curves for cores 343340-6-1 (upper) and DA00-06 (lower) with some radiocarbon dates. The cores appear to reflect a common sequence of events, as demonstrated by the lines connecting features identified as originating from the same event. The interval between dates show that the accumulation rate was very high in the lower half of the core, and significantly lower in the upper half. Based on Lloyd *et al* (2005) and data provided by Lloyd via personal communication.

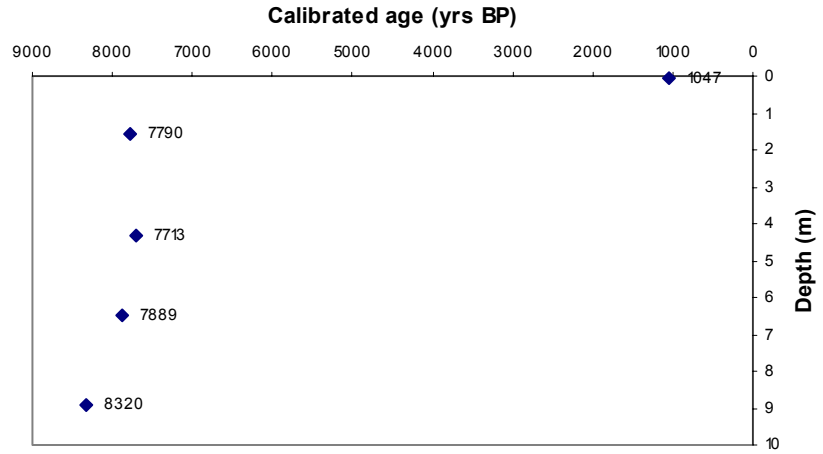

Fig. 19. Age-depth diagram for the correlated core DA00-06, used to evaluate the age-model. The age values are based on radiocarbon analysis on foraminifers and bivalves in Lloyd *et al*. (2005).

be seen in fig. 16. It shows a steady increase in chlorine through the entirety of the sediment core. This could however be an effect caused by lower sediment density and increased sea-water content, as suggested by Tjallingii et al. (2007).

4.5 Dating the core

The only radiocarbon date available at the time of writing for core 343340-5-1 gives a ^{14}C age 2 550 yr BP at a depth of 55 cm (POZ-22361, 2555± 30 BP at 53-58cm depth (Snowball, personal communication)). Magnetic susceptibility correlation with core DA00-06 in Lloyd *et al.* (2005) as seen in fig. 18, suggests that the examined core 343340-6-1 contains material from approximately the past 8.5 kyr BP. It further shows a great variability in accumulation rates. The upper 8 meters of DA00-06 contains material from approximately 8.3-7.8 kyr BP. The upper 150 cm would display dramatically lower sedimentation rates, as it was deposited over approximately 6 000 years. The radiocarbon datings performed by Lloyd *et al.* (2005) were obtained from both foraminifers and bivalves. It is notable that the date indicating 7 713 yr BP was obtained from bivalves. It gives a younger age than the foraminiferal datings which provided the date for 7 790 yr BP, although it is located further down in the core.

The age-depth diagram in fig. 19 shows the relationship of the given ages against the depth of the core. The observations made in the correlation diagram regarding changes in sedimentation rates become even clearer. The earliest four ages, stretching over 530 yrs, would have accumulated as much as 80 % of the sediment column, while the uppermost meter would have taken 7 kyr to form.

5. Discussion

The major aims of the study, which were to discern sections of enhanced haematite-levels within the core and draw connections to ocean current variations, were met. Due to the lack of radiocarbon ages from the examined core (only one date is currently available from a parallel core) the dating control is poor. It is therefore difficult to make any certain connections between the retrieved data patterns and past climate variations. An improved age-model would enable future investigations to compare local climate records from a number of sources, with magnetic data obtained in this study. This could be an important step towards a further understanding of the interaction between climate change, ocean currents and the response of the Greenland ice sheet in the near vicinity of Disko Bugt.

The magnetic mineral identification was initially attempted by means of comparison with literature data for pure minerals. As the samples consisted of magnetic assemblages with a variety of different sources and dilution from non-magnetic phases, a perfect match cannot be expected. The difficulties with identifying accurate and relevant signatures leave many opportunities for misinterpretations, but as the number of bedrock types in Disko Bugt region are limited, the risk of misidentification should be considered moderate. It is not possible within the limits of this investigation to achieve any higher degree of detail and this is perhaps not very meaningful either as the study is based on one single core. The large-scale events and trends should nevertheless be detectable in the material, and conclusions can be drawn about environmental events by comparing the results with other studies from the area.

The large fluctuations in magnetic susceptibility in the lower half of the core are likely to be caused by individual grains of coarse ice-rafted debris (IRD), which are not representative of the bulk sediment. The sharp, individual peaks are thought to be large stones in the core, which can give rise to very high susceptibility values if they are close to the sensor. Underneath these sharp peaks a general baseline, respresentative of the bulk sediment, can still be identified. This is especially clear when considering the SIRM/χ diagram in fig. 10e and 11.

Low values of S_{-100}, below -0.8, are interpreted as a section with enhanced levels of magnetite, as this mineral will give rise to more negative S-ratios than those for haematite. The slightly lower values before and after this section can signify a higher iron-content, which could be indicative of more haematite. The presumed elevated levels of magnetite coincide with increased magnetic susceptibility. Comparing the S_{-100}-ratio diagram with the diagram showing magnetic susceptibility, it is clear that the susceptibility plateau is located in the same position as the S_{100}-trough. This interpretation gains some support from the SIRM. As is shown in the SIRM diagram in fig. 10c, the bulk of the values remain in the vicinity of 15-25 Am^2/kg for samples below about 300 cm. These figures are compatible with a dominating content of magnetite in the sediments, according to table 1 and the S_{-100} ratio.

The comparison between magnetic susceptibility and the SIRM/χ reveal relatively elevated levels of haematite present mainly in the interval 925-700. This is the interval where the SIRM/χ is lifted compared to the susceptibility curve. Areas where the susceptibility curve is higher than the SIRM/χ would then be interpreted as being dominated by magnetite. The aforementioned trough in the S_{100} diagram can be correlated to a trough in the SIRM/χ diagram, which verifies this method as they are both interpreted as magnetite-rich sections.

HIRM is traditionally used to detect the presence of hard magnetic materials such as haematite. At levels of -100 mT however, it is unlikely that all the magnetite has been saturated, particularly if grains are

small and elongated. This should, however, be the case at -300 mT. Therefore, the difference between $HIRM_{100}$ and $HIRM_{300}$ could be used to show the presence of "hard" magnetite due to grain size sorting versus haematite. The most significant area of differing values is found in Zone II, where $HIRM_{100}$ displays several peaks, which include the maximum values for the curve. The $HIRM_{300}$ for the corresponding area remains largely passive, apart from the small interval around 513-518 cm, where a distinct peak is seen. This peak appears to be an isolated occurrence and does not take any part in the long-term trends. Minerals with magnetic properties which would place them in between haematite and magnetite and thus interfere with this interpretation method, such as the ferrimagnetic iron sulphide greigite, are not expected to be found in any significant quantities in the area.

A comparison between the curves for magnetic susceptibility and SIRM/χ and those for HIRM can further clarify the picture. The large peak in the SIRM/χ diagram, which is located in Zone II, would be interpreted as a sudden presence of haematite within a trough representing magnetite, and can be explained using the HIRM information. It is clear that this area does not coincide with a peak in haematite due to the low $HIRM_{300}$ values. The $HIRM_{100}$ further shows the very same peak, giving the conclusion that it is hard magnetite which is responsible for the sudden rise. Zone II therefore remains largely dominated by magnetite.

A comparison between the curves in fig. 12 further supports this conclusion. The two parameters used, SIRM/χ and χ_{ARM}/SIRM, can both be used as magnetic grain size indicators. Correlations with other curves reveal that the peak at around 500 cm can be due to a reduction in magnetic grain size. This would be consistent with previous interpretations, and also give further support to those conclusions. The peak seen in the SIRM, SIRM/χ and $HIRM_{100}$ diagrams could be interpreted as a sign of the 8.2 event, but without proper dating that conclusion can not be substantiated.

Due to the geological setting of the core site, the sediment can be expected to be magnetically dominated by magnetite from proximal basalt sources. There will also be a certain input of haematite-rich sediment from the sedimentary bedrock from the inner Disko Bugt. Sections with elevated haematite levels will, according to the hypothesis, occur at times when the WGC in the bay is strong enough to move icebergs through the Vaigat strait and bring sedimentary rock material (as IRD) from there to the deposition site. During the LGM and possibly through the late-glacial and early post-glacial periods, Disko Bugt itself was partially covered by the ice sheet. The retreat dates given by fig. 5, show that the ice-margin was relatively far out in the bay as late as 10 kyr BP, while the dates provided by core DA00-06 (and correlated to 343340-6-1), show that the earliest part of the core is probably not older than 8.5 kyr.

The implications are, however, that icebergs would - at times when the WGC was either too weak or the northern passage blocked - travel along a path to the west (see fig. 4 for icebergs paths traced by scouring marks on the sea bottom). If this scenario is applied to the time of deposition for the examined core, it could mean that strong meltwater flows could use the same path. Sediment at the core site would then be completely dominated by material from the mainly basaltic areas of southern and western Disko Bugt, which would result in higher magnetite levels.

Preliminary findings from analyses performed on a parallel core to 343340-6-1, are described in Dietrich *et al.* (2007). XRF data show a pattern of elevated levels of sulphur and declining amounts of titanium as well as a drop in magnetic susceptibility. These changes have been interpreted as a signal of higher organic production, caused by a retreat of the ice margin and increasing influence of warmer WGC in the area. The titanium is thought to have been eroded from the bedrock of mainland Greenland by glacial forces. The higher levels of titanium that were observed in the lower parts of the core show the opposite relationship, which would indicate a more proximal ice-margin. The XRF data from the upper 200 cm of core 343340-6-1 are not sufficient to establish any such trend. As the cores were taken from the same site, however, it is deemed reasonable to assume that the major trends are the same. Furthermore, the increased influx of sulphur may be caused by the higher concentrations organic material in the upper parts of the core. As the rate of organic material becomes higher, the relative amount of magnetic sediment will decrease. This could reasonably account for the general downturn in all magnetic properties in the upper 400 cm of the core. It appears likely that this development could mark the beginning of the Holocene.

The implications of the interval of higher haematite in Zone I could be that at the time of these deposits there was a strengthened WGC, carrying more material past the sedimentary bedrock areas, through the Vaigat strait. Here the water would have been enriched with relatively haematite-rich sediments. This gains some support from the XRF results of the parallel core. A drop in iron is seen to coincide with the central trough in the SIRM/χ diagram. This could be related to a drop in iron-rich haematite in the sediments.

The above scenario implies that the Vaigat strait was ice-free during the formation of Zone I. A combination of relatively low ice-levels in the bay and a strengthened WGC shows that warmer conditions were prevalent at times of enhanced haematite levels in the sediment. Lloyd *et al.* (2005) discuss a scenario which is compatible with this, where the Jakobshavn Isbrae ice-stream retreated eastwards in a second wave after the initial deglaciation at ca 9.2 kyr BP. This is thought to have led to a reduction in the amount of meltwater discharge to the bay, allowing the WGC to penetrate into the Disko Bugt. The absence of a direct

westerly meltwater current flowing through the southern inlet to the bay, could also allow a stronger WGC entering Disko Bugt. Another argument for the increasingly warmer conditions that signify Zone I is the presence of mottling in the sediments at levels around 950 cm. Such mottling is a sign of bioturbation and would be the earliest indication biological activity observed in the core. No shells have been identified below 700 cm, but the lithological description of parallel core 343340-5-1 in Dietrich *et al.* (2007) does include shells at levels below 10 m.

The section of the core with enhanced levels of magnetite (mainly Zone II) would then reasonably indicate a weaker WGC in Disko Bugt. The material would then come primarily from sources in outer Disko Bugt, thus being of mainly basaltic origin. This is also supported by Lloyd *et al.* (2005), where the palaeoceanography of Disko Bugt during the early Holocene is discussed. The conclusions drawn in that paper show that the warm waters of the WGC were diverted from the eastern parts of Disko Bugt by the large amounts of meltwater from the ice-streams. This process continued until ca 7.8 kyr BP and is identified as the downturn in magnetic susceptibility seen in core DA00-06, and reflected in Zone III of core 343340-6-1. Zone II furthermore marks the first occurrence of shells found in the sediment at around 700 cm. The notable absence of biological activity between the area with mottling in Zone I and the shell fragments in Zone II could be due to the GH-8.2 cooling event. Although this major climate turnover did not have any significant impact on the geomorphology of the area, it would be expected to have had a dramatic impact on the fauna. Such a conclusion is speculative and is not supported by the lithological description of parallel core 343340-5-1 as given by the cruise report, as shells have been observed further down in that core (Dietrich *et al*., 2007).

The upper part of Zone IV shows a sharp peak in both S-ratios and HIRM, which could be identified as a sudden input of haematite. The reason for this sudden, dramatic event is open for speculation. The event is relatively recent, occurring in the vicinity of 2 kyr BP. The XRF analyses do not appear to show any compatibility between any examined element and the event. The magnetic susceptibility of parallel core 343340-5-1 does have a minor peak at the same depth, although it is much less pronounced. Similarly, data from core DA00-06 show a sharp, but short-lived and isolated peak on the same spot. It is conceivable that the event causing the peaks does not signify any major climate shift in the region. The past 3 000 years does include several shifts in the climatic conditions, as mentioned in e g Moros *et al.* (2004). It is nonetheless thought that there is as of now insufficient evidence to relate the dramatic events of Zone IV to any known environmental occurrence.

From the biplots presented in figures 13, 14 and 15 it is clear that Zones III and IV are distinctly different in their magnetic composition from Zones I and II. It is plausible that this is related to the overall decrease in the levels of magnetic material in these zones. There is, however, a risk of over interpreting changes in magnetite and haematite ratios, as the change in organic sediment input may have a major impact on their absolute concentrations. The reliability of the magnetic record for Zone IV is further compromised by the presence of mottling. As the sediments have been bioturbated, the magnetic patterns as they were deposited may have been altered and smoothed to different degrees Thus, a comparison with multiple parallel cores would be useful to validate this part of the magnetic record.

The clear distinction between levels of differing magnetic characteristics in the biplots in figures 13, 14 and 15 further demonstrates the usefulness of those parameters. The division between magnetite- and haematite-enriched sediments in fig. 13 also supports the interpretation that these two sections represent areas of differing mineral content.

The notable absence of any significant response to the GH-8.2 cooling event in the material, which could be expected to take place in Zone I (according to the age-model), reflects conclusions drawn by Long *et al.* (2006), where no ice-margin response to this event could be detected in Disko Bugt. However, independent dating control is lacking

The radiocarbon ages given are not entirely consistent as they were measured using both bivalves and foraminifers, which may have ^{14}C signatures of different water masses. One level was noted to be attributed a younger age than an overlying level. The intervals for those ages overlap although they are 200 cm apart, illustrating the rapid sedimentation rate in the lower parts of the core. The fact that the age-depth diagram appears to show a good consistency for carbon dates from foraminifers, but not so for dates analysed on bivalves could be due to a re-deposition of the bivalves. The location of the correlated core DA00-06 inside Disko Bugt could have brought plenty of opportunity for the sediments to be re-deposited, or even for parts of it to have been removed. The choice of the coring site for core 343340-6-1 may have been influenced by the desire to get a continuous record, and to avoid the risk of getting a hiatus. By choosing a coring site some distance away from the major sediment sources, this should be possible to achieve. If the age of 7 790 yrs BP was correct, that would mean that 5 meters of the core were deposited in the span of only 100 years. This would assume an almost ten-fold increase in the sedimentation rate from 5.6 mm/year between 8.91-65 m, to 49 mm/year in the interval 65-159 m. If a different age model is chosen instead, disregarding the suspected misleading age value, the upper 4 meters would instead have taken 7 000 years to form, with a more reasonable sedimentation rate of 0.64 mm/yr.

The correlation between the two cores could also be somewhat misleading, as core DA00-06 was obtained further inside the bay, in closer proximity to

the ice-margin. This means that the corresponding features in the magnetic records of DA00-06 and 343340-5-1, could have occurred at different points in time as ice either advanced or retreated.

The data and results from a few or even a single point of a "restricted" area, such as the Disko Bugt, can by no means give but a fragment of a hint to the dramatic and shifting climatic conditions over the whole of Greenland. It is only when analyses on a large number of marine and terrestrial sequences have been performed that the full picture will begin to appear. Further research into the intricate web of climate-controlling interactions is of dire need in these times of a "looming climate threat". Environmental magnetism has been shown to be a useful tool indeed, and can provide valuable clues about past environmental events. A further technological and methodological development that will make the method more accessible and accurate will surely give rise to new applications and open up new fields of research. Evermore subtle pieces of information, made available by new technology, will sharpen the focus of the picture of the past, and further our understanding of our world and its behaviour.

6. Conclusions

- Elevated levels of haematite are interpreted as an indicator of a stronger WGC, transporting material from the sedimentary bedrock deposits on its path through the Vaigat strait.

- Levels lacking a significant haematite content are thought to represent times of a weaker WGC regime, possibly due to a higher discharge of glacial meltwater into the bay. A less powerful WGC would have limited ability to transport any large amounts of material out to the periphery of the bay. The sediments would be dominated by material of local, mainly basaltic origin.

- Zone I: This zone is dominated by IRD deposits, as indicated by the strong, rapid fluctuations in the magnetic record. Elevated levels of heamatite have been identified in the upper part of this zone, marking an increased influence of the WGC in Disko Bugt.

- Zone II: A magnetic susceptibility plateau represents relatively high levels of magnetite in this zone. As mentioned by Lloyd *et al.* (2005), this perceived weakening of the WGC is explained by an increase in meltwater discharge, pushing the WGC westwards.

- Zone III: An overall decrease in magnetic material in the sediment, likely due to a higher organic production as seen in sulphur curves from XRF analyses. This can be interpreted as the advent of the Holocene.

- Zone IV: This zone is characterised by several large shifts in magnetic susceptibility. A few peaks of what is interpreted as high haematite levels are identified in the uppermost part of the core. No satisfactory explanation for the event can be given at this time. The suddenness and short durability of it does raise suspicion that it could be a local interference with no connection to regional environmental occurrences.

7. Acknowledgments

I would like to thank my head supervisor Ian Snowball for his excellent support during the work on this project, and co-supervisor Per Sandgren for his time and efforts. Important input has also been provided by Jerry Lloyd of Durham University and Andreas Nilsson. I also gratefully acknowledge the contributions from Oskar Jäckel whose cooperation during the initial laboratory work was much appreciated, and who performed the XRF analyses in Stockholm, Finally I would like to thank all the staff and students at the Department of Geology in Lund for their support over the years.

8. References

Bennike, O. & Björck, S., 2002: Chronology of the last recession of the Greenland ice sheet. *Jour nal of Quaternary Science 17*, 211-217.

Bennike, O., Hansen, K. B., Knudsen, K. L., Penney, D. N. & Rasmussen, K. L., 1994: Quaternary marine stratigraphy and geochronology in cen tral West Greenland. *Boreas 23*, 194-215.

Birkelund, T., 1971: Mesozoikum or tertiær. In Nørre vang, A., Meyer, T. J. & Christensen, S. (editors) *Danmarks Natur Bind 10: Grønland og Færøerne*, 87-109. Politikens Forlag.

Brett, C. P. & Zarudzki, E. F. K., 1979: Project West mar, a shallow marine geophysical survey on the West Greenland shelf. *Rapport Grønlands geologiske undersøgelse 87*, 27.

Buch, E., 1981: The annual cycle of temperature, sa linity, currents and water masses in Disko Bugt and adjacent waters, West Greenland. *Med delelser om Grønland Bioscience 5*, 1-33.

Butler, F., 1992: *Paleomagnetism: Magnetic domains*

to geologic terranes. Blackwell Scientific Pub lications, Boston. 319 pp.

Chalmers, J. A., Pulvertaft, T. C. R., Marcussen, C. & Pedersen, A. K., 1999: New insight into the structure of the Nuussuaq Basin, central West Greenland. *Marine and Petroleum Geology 16*, 197-224.

Dietrich, R., Endler, R., Harff, J (ed.)., Hentzsch, B., Jensen, J. B., Kuijpers, A., Krauss, N., Leipe, T., Lloyd, J., Mikkelsen, N., Moros, M., Nickel, G., Perner, K., Richter, A., Risgaard-Petersen, N., Rysgaard, S., Richter, T., Sandgren, P., Sheshenko, V., Snowball, I., Trost, E., Waniek, J., Weinrebe, W. & Witkowski, A., 2007: *Cruise Report R/V Maria S. Merian Cruise MSM 05/03, June 15 to July 4, 2007 from Nuuk to Nuuk.* 169 pp.

Evans, M. E. & Heller, F., 2003: *Environmental Mag netism – Principles and Applications of Enviro magnetics*. Academic Press, 299 pp.

Garde, A. A. & Steenfelt, A., 1999: Precambrian geol ogy of Nuussuaq and the area north-east of Disko Bugt, West Greenland. In Precambrian geology of the Disko Bugt region, West Greenland. ed. Kalsbeek, F. *Geology of Greenland Survey Bulletin 181*, 7-40.

Henriksen, N., Higgins, A. K., Kalsbeek, F. & Pulver taft, T. C. R., 2000: Greenland from Archaean to Quaternary: Descriptive text to the Geologi cal map of Greenland, 1:2 500 000. *Geology of Greenland Survey Bulletin 185*, 93 pp. + map.

Ingólfsson, Ó., Frich, P., Funder, S. & Humlum, O., 1990: Paleoclimatic implications of an early Holocene glacier advance on Disko Island, West Greenland. *Boreas 19*, 297-311.

Kuijpers, A., Lloyd, J. M., Jensen, J. B., Endler, R., Moros, M., Park, L. A., Schulz, B., Gutfelt Jen sen, K. & Laier, T., 2001: Late Quaternary cir culation changes and sedimentation in Disko Bugt and adjacent fjords, central West Greenland. *Geology of Greenland Survey Bul letin 189*, 41-47.

Larsen, J. G. & Pulvertaft, T. C. R., 2000: The struc ture of the Cretaceous-Palaeogene sedimentary-volcanic area of Svartenhuk Halvø, central West Greenland. *Geology of Greenland Survey Bulletin 188*, 44.

Lloyd, J. M., 2006: Late Holocene environmental change in Disko Bugt, west Greenland: interact tion between climate, ocean circulation and Jakobshavn Isbrae. *Boreas*. *35*, 35-49.

Lloyd, J. M., Park, L. A., Kuijpers, A. & Moros, M., 2005: Early Holocene palaeoceanography and deglacial chronology of Disko Bugt, West Greenland. *Quaternary Science Reviews 24*, 1741-1755.

Lloyd, J. M., Kuijpers, A., Long, A., Moros, M. & Park, L. A., 2007: Foraminiferal reconstruction of mid- to late-Holocene ocean circulation and climate variability in Disko Bugt, West Greenland. *The Holocene 17:8*, 1079-1091.

Long, A. J. & Roberts, D. H., 2003: Late Weichselian deglacial history of Disko Bugt, West Greenland, and the dynamics of the Jakob shavns Isbrae ice stream. *Boreas 32*, 208-226.

Long, A. J., Roberts, D. H. & Dawson, S., 2006: Early Holocene history of the west Greenland Ice Sheet and the GH-8.2 event. *Quaternary Sci ence Reviews 25*, 904-922.

Long, A. J., Roberts, D. H. & Rasch, M., 2003: New observations on the relative sea level and degla cial history of Greenland from Innaarsuit, Disko Bugt. *Quaternary Research 60*, 162-171.

Maher, B. A., Thompson, R. & Hounslow, M. W., 1999: Introduction. In Maher, B. A. & Thomp son, R. (editors) *Quaternary Climates, Environ ments and Magnetism*, 1-48. Cambridge Uni versity Press, Cambridge.

Moros, M., Emeis, K., Risebrobakken, B., Snowball, I., Kuijpers, A., McManus, J. & Jansen, E., 2004: Sea surface temperatures and ice rafting in the Holocene North Atlantic: climate influ ences on northern Europe and Greenland. *Qua ternary Science Reviews 23*, 2113-2126.

Oldfield, F., 1999: The rock magnetic identification of magnetic mineral and magnetic grain size as semblages. In Walden, J., Oldfield, F. and Smith. J. P. (editors) *Environmental Magnet ism: A Practical Guide*, 98-112. Quaternary Research Association, London.

Rasch, M., 1997: A compilation of radiocarbon dates from Disko Bugt, central West Greenland. *Geografisk Tidsskrift 97*, 143-151.

Reeh, N., 1994: Calving from Greenland glaciers: ob servations, balance estimates of calving rates, calving laws. In Reeh, N. (ed.), *Report on the workshop on the calving rate of West Greenland glaciers in response to climate change*, 85-102. Danish Polar Center, Univer sity of Copenhagen, Copenhagen.

Roberts, D. H. & Long, A. J., 2005: The marginal sub glacial signature of Jakobshavn Isbrae, West Greenland: implications for ice stream and ice sheet dynamics. *Boreas 12*, 211-222.

Snowball, I. F., 1993: Geochemical control of magnet ite dissolution in subarctic lake sediments and the implications for environmental magnetism. *Journal of Quaternary Science 8*, 330-346.

Snowball, I., 1999: Electromagnetic units and their use in environmental magnetic studies. In Walden, J., Oldfield, F. & Smith. J. P. (editors) *Environ mental Magnetism: A Practical Guide,* 89-97. Quaternary Research Association, London

Thompson, R. & Oldfield, F., 1986: *Environmental Magnetism*. Allen and Unwin Ltd, London, 227 pp.

Tjallingii, R., Röhl, U., Kölling, M. & Bickert, T., 2007: Influence of the water content on X-ray fluorescence core-scanning measurements in soft marine sediments. *Geochemistry Geophys*

ics Geosystems 8:2, 1-12.

Walden, J., 1999: Remanence measurements. In Wal den, J., Oldfield, F. & Smith. J. P. (editors) *Environmental Magnetism: A Practical Guide,* 63-88. Quaternary Research Association, Lon don

Warren, C. R. & Hulton, N. R. J., 1990: Topographic and glaciological controls on Holocene ice-sheet margin dynamics, central West Greenland. *Annals of Glaciology 14*, 307-310.

Weidick, A. & Bennike, O., 2007: Quaternary glacia tion history and glaciology of Jakobshavn Isbræ and the Disko Bugt region, West Greenland: a review. *Geological Survey of Denmark and Greenland Bulletin 14*, 80 pp.

Weidick, A., Oerter, H., Reeh, N., Højmark Thomsen, H. & Thorning, L., 1990: The recession of the Inland Ice margin during the Holocene Climatic optimum in the Jakobshavn Isfjord area of West Greenland. *Palaeogeography, Palaeoclimatol ogy, Palaeoecology 82*, 389-399.

Appendix 1

Protocol of the seven parallel cores 343340 acquired during the June 2007 scientific cruise with R/V Maria S. Merian (Dietrich *et al* 2007). The core which this study focuses on is the number six in the sequence.

Projekt: Cruise: MSM 05/3

RV- Stat. Code	RV MSM	Area Disco Bay	Year 2007	Month June	Day 20	Start (UTC) 10:30:15	IOW- Station ID 343340
Lat. 68°23,838' Long. 55°7,790'	Water depth start 460,35	Station description No. Of Cores: 16 MUC; 3 GC Positioning System: GPS Geoid: WGS84 Stationsname:					
Core	Time (UTC)	Real Position Lat. Long.	Depth (m)	Gear	Corerlength (m)	Penetration / Gain (m)	Scientist/ Institute	Comment
-1	10:37:32	68°23,837' 55°07,787'	460,65	CTD			Waniek (IOW)	
-2	11:32:40	68°23,836' 55°07,786'	467,60	MUC	0,6	0,34	Moros, Endler (IOW) Mikkelsen (GEUS) Rysgaard (GINR) Lloyd (UD)	#1 Moros (sliced) MagSus done onboard #2 Endler #3-8 subsampled by Lloyd, Mikkelsen, Rysgaard
-3	12:27:33	68°23,837' 55°07,786'	462,75	MUC	0,6	0,34	Witkowski (US) Mikkelsen (GEUS)	#1-8 subsampled by Witkowski,
							Rysgaard (GINR)	Mikkelsen, Rysgaard
-4	13:14:02	68°23,837' 55°07,786'	463,1	GC	6 (foil)	Ca. 6 m	Rysgaard (GINR) Mikkelsen (GEUS)	subsampled by Rysgaard, Mikkelsen
-5	14:18:35	68°23,835' 55°07,779'	461,2	GC	12 (liner)	10,74	Moros (IOW) Snowball (GBSC) Richter (NIOZ)	MagSus and XRF done onboard
-6	15:34:46	68°23,834' 55°07,773	461,3	GC	12 (liner)	11	Endler (IOW) Sandgren (GBSC)	After MSCL to Lund
-7				GPS-buoy			Dietrich (TUD)	

Appendix 2

Seismic profile of coring station 343340 (marked in the figure), stretching approximately from west to east (Dietrich *et al*., 2007).

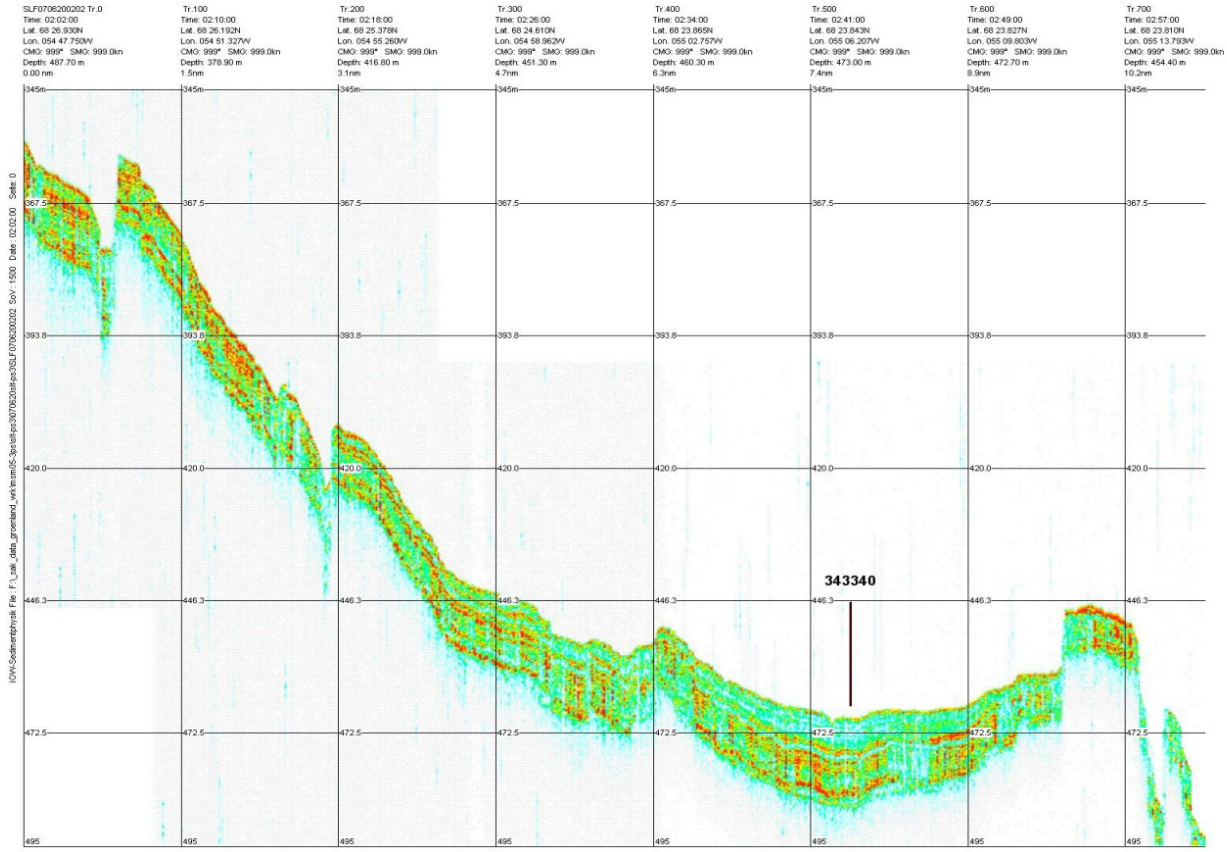

Appendix 3

Lithological description of the individual core sections based on ocular inspection.

Depth (cm)	***Lithological description***
101-0	Moderate olive brown clay with minor amounts of silt. Olive grey mottling prominent at 95-55 cm, and again at 22-0 cm.
201-101	Medium olive brown, modestly silty clay. Interval with numerous shell fragments at 148-132 cm.
301-201	Slightly silty clay with black stains identified as coal fragments. Interval with numerous shells at 279-226 cm. Gradual transition from moderate olive brown towards medium olive brown.
401-301	Slightly silty clay. Gradual transition from light olive grey to moderate olive brown towards the top. Few shell fragments.
501-401	Light olive grey silty clay with occasional shell fragments and black spots identified as fragments of coal.
601-501	Light olive grey silty clay with occassional shell fragments and bits of coal.
702-601	Light olive grey silty clay with occasional shell fragments and bits of coal. Shells noted at 695, 655 and 651 cm.
803-702	Light olive grey silty clay with traces of sand. Fragments of coal 1-2 mm at 732 and 749 cm. Unidentified brown stain at 784 cm. Dropstone at 750 cm.
904-803	904-870 cm gradual transition to light olive grey silty clay. Above the transition zone, 870-803 cm, light olive grey clay. Occasional dropstones, including one with an estimated diameter of 8 cm at 880 cm.
1004-904	1004-955 cm medium grey – olive grey, banded silty clay. 955-939 cm medium grey -olive grey clay with mottling. 939-935 cm mottling seizes, banding resumes. 939-904 medium grey - olive grey clay with mottling.
1104-1004	Medium grey – olive grey, banded silty clay. Centimetre-scale, olive grey laminations. 3-4 cm dropstone at 1038 cm.

Appendix 4

Equipment used in this study. The analytic work was performed at the Palaeomagnetic and Mineral Magnetic Laboratory at the Department of Geology in Lund.

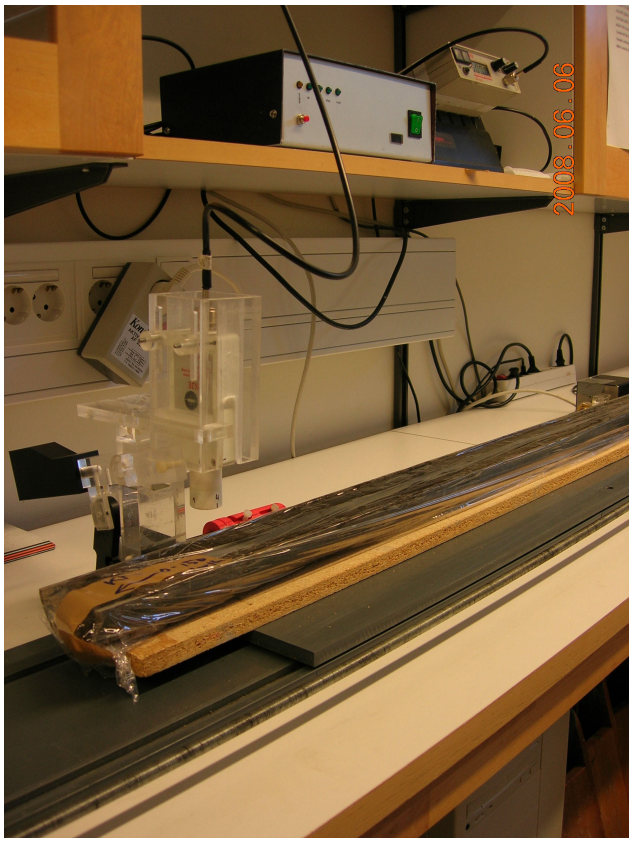

Fig. 20. Tamiscan TS-1 automatic conveyor system, equipped with a Bartington MS-2E sensor.

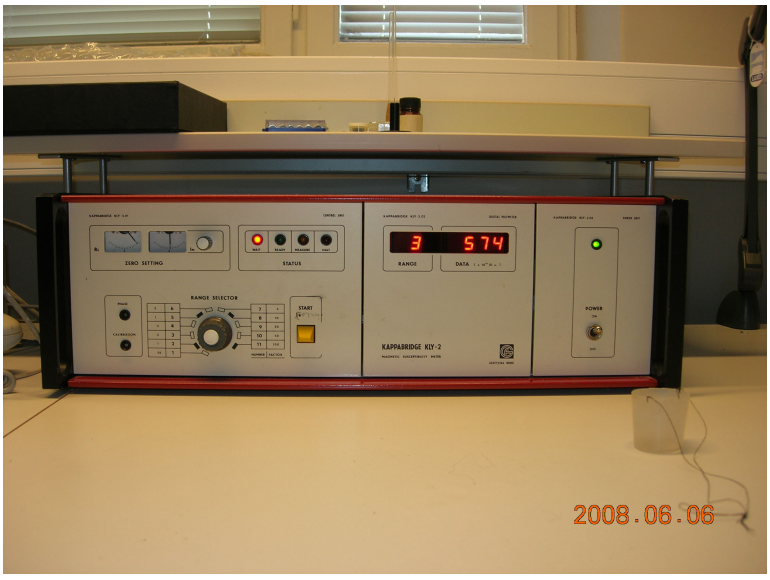

Fig. 21. Geofyzica Brno KLY2 Kappabridge device, used for measuring magnetic susceptibility on the subsamples.

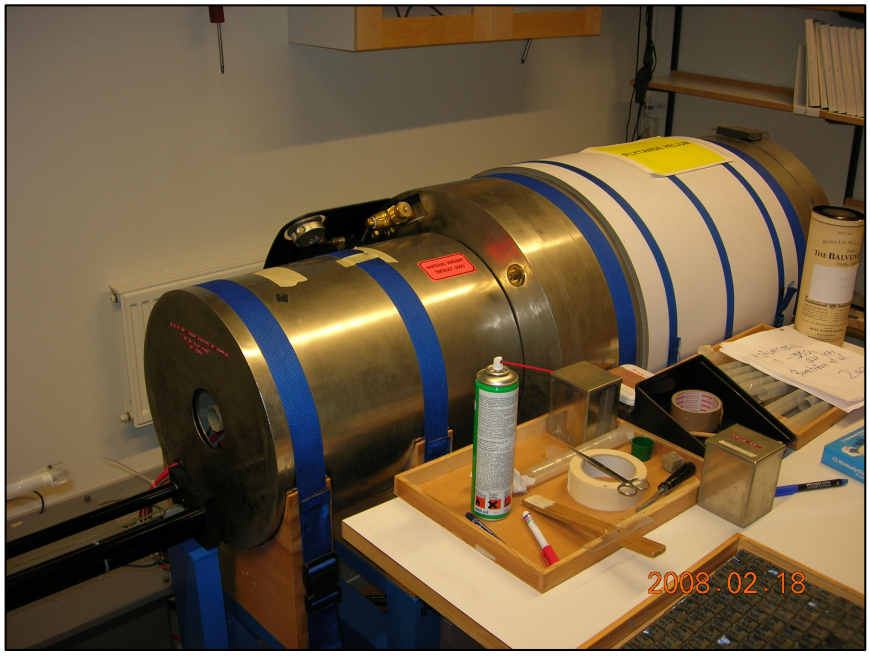

Fig. 22. The ARM-field was acquired with an Enterprises model 615, using a field strength of 100 mT.

Fig. 23. Radcliffe 700 pulse magnetiser, used for applying both SIRM and IRM.

Fig. 24. The Molspin pulse magnetiser, used for producing the –100 mT IRM.

Fig. 25. A Molspin magnetometer.

Appendix 5

XRF diagrams for the relevant analysed elements silicon, potassium, calcium, titanium, iron, manganese, barium and boron. The analysis was carried out on the upper 200 cm of the examined core 343340-6-1 at the department of Earth sciences, Stockholm university.

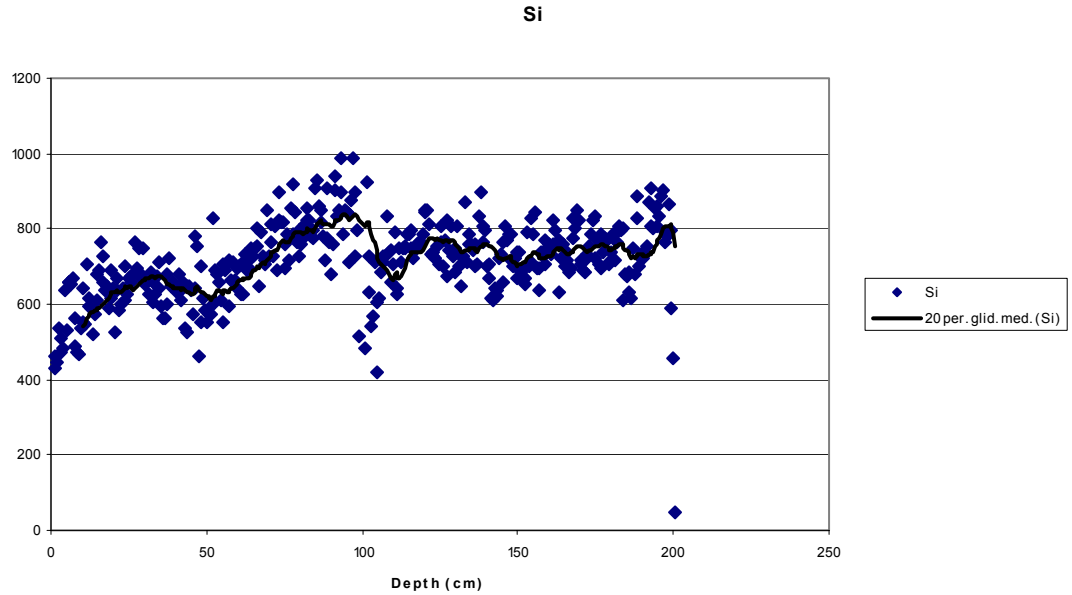

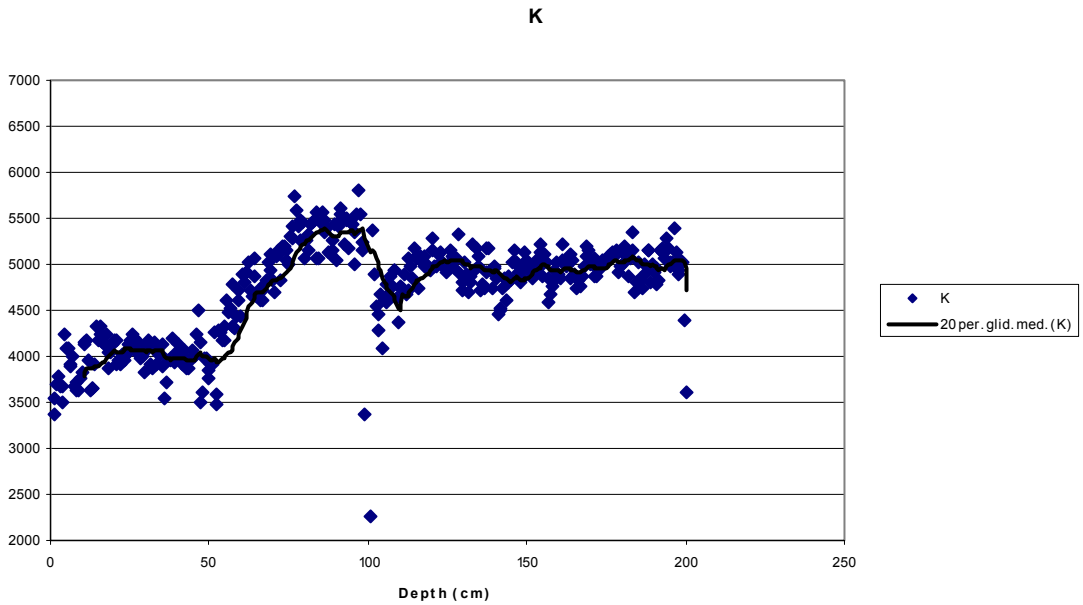

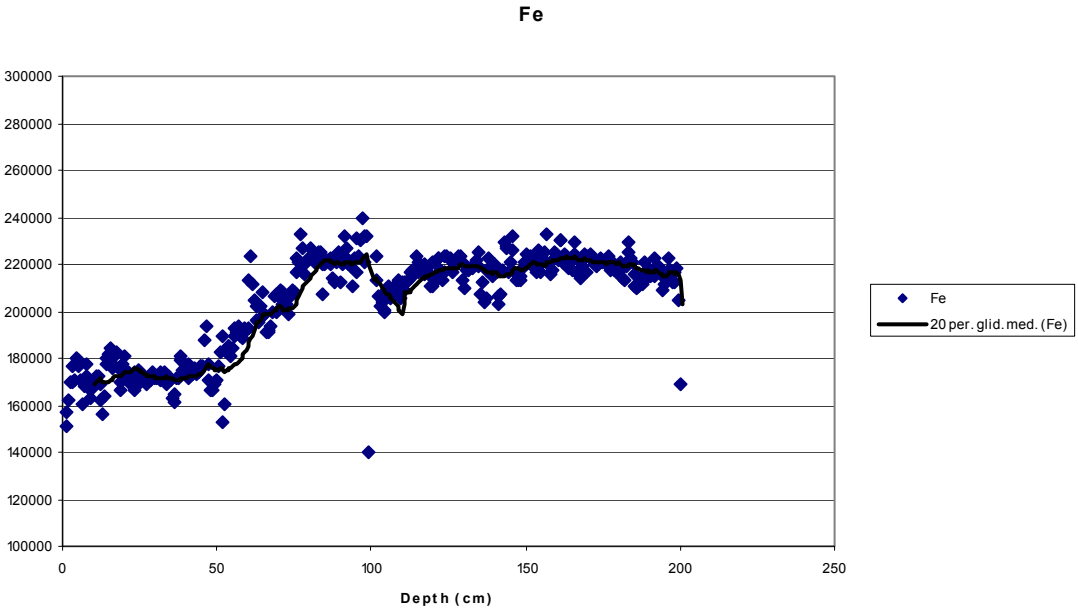
Fe
300000
280000
260000
240000
220000
200000
180000
160000
140000
120000
100000
0
50
100
150
200
250
Depth (cm)
Fe
20 per. glid. med. (Fe)

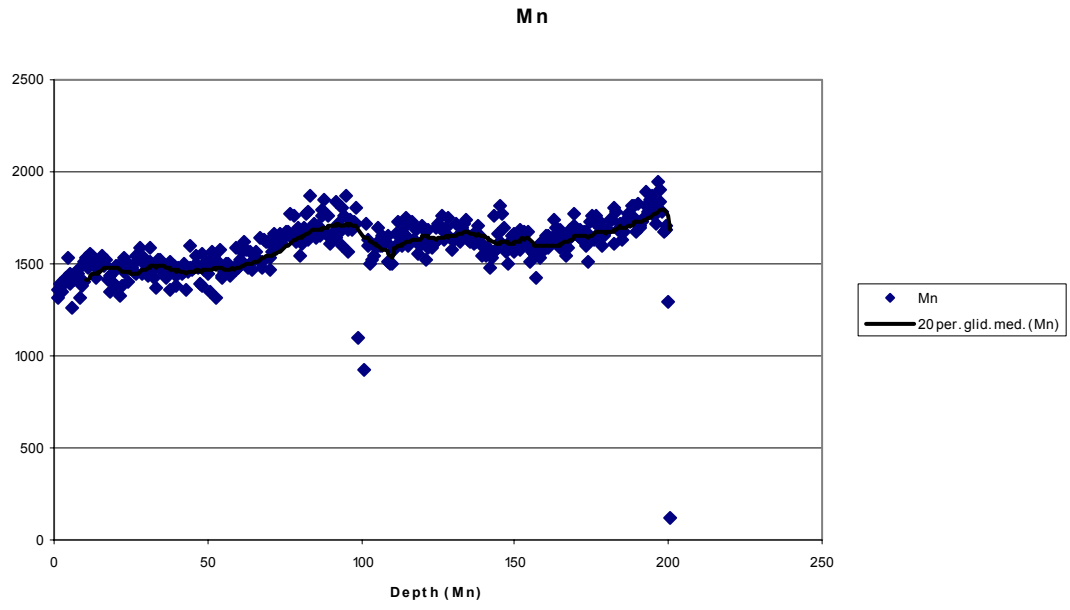
Mn
2500
2000
1500
1000
500
0
0
50
100
150
200
250
Depth (Mn)
Mn
20 per. glid. med. (Mn)

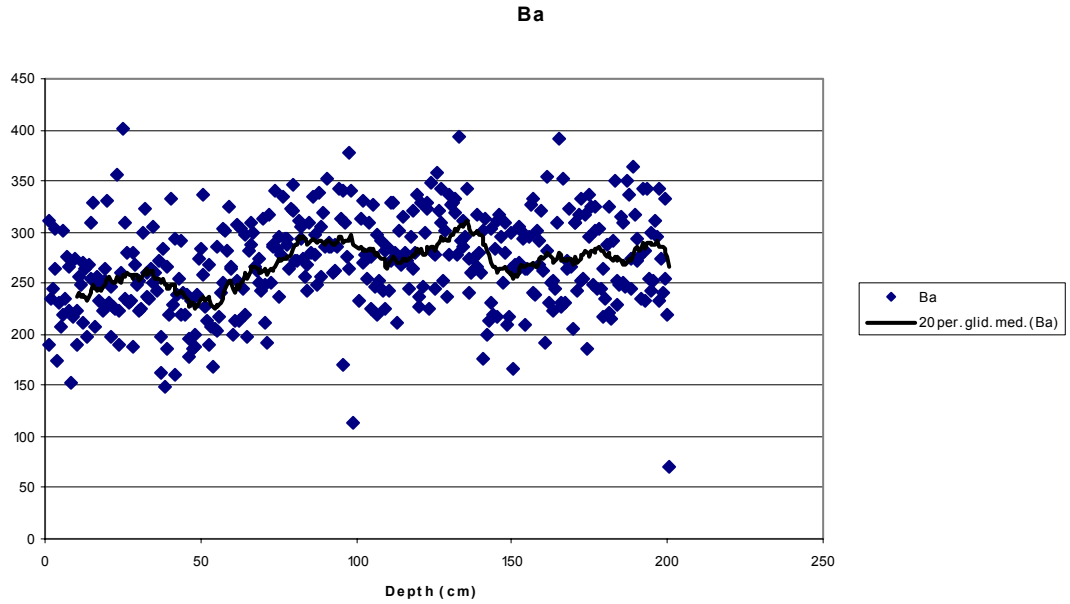
Ba
450
400
350
300
250
200
150
100
50
0
0
50
100
150
200
250
Depth (cm)
Ba
20 per. glid. med. (Ba)

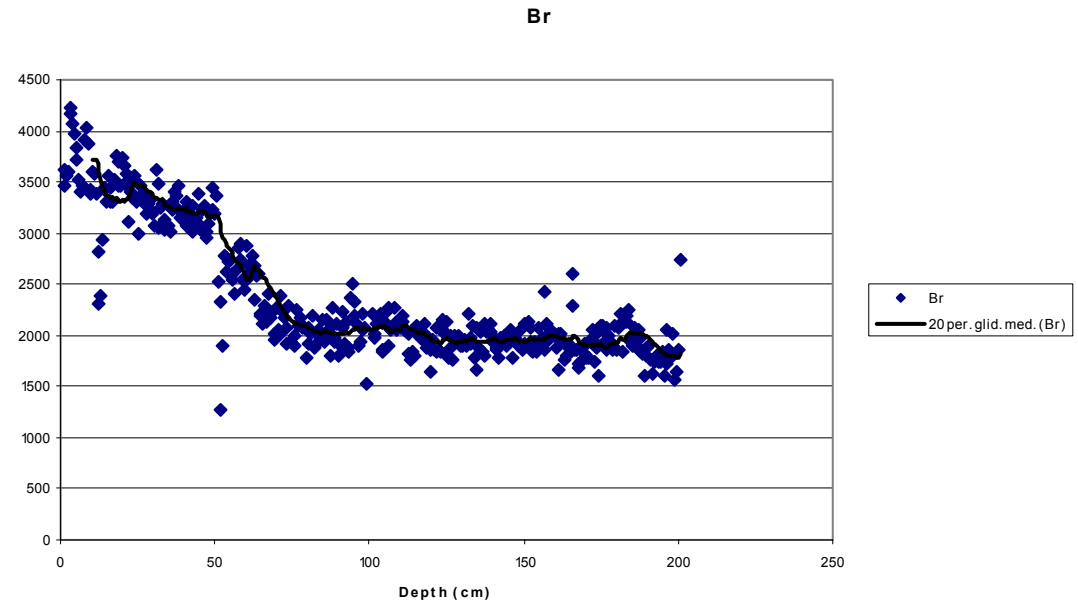
Br
4500
4000
3500
3000
2500
2000
1500
1000
500
0
0
50
100
150
200
250
Depth (cm)
Br
20 per. glid. med. (Br)

Tidigare skrifter i serien ”Examensarbeten i Geologi vid Lunds Universitet”:

188. Nilsson, Eva K., 2005: Extinctions and faunal turnovers of early vertebrates during the Late Silurian Lau Event, Gotland, Sweden.
189. Czarniecka, Ursula, 2005: Investigations of infiltration basins at the Vomb Water Plant – a study of possible causes of reduced infiltration capacity.
190. G³owacka, Ma³gorzata, 2005: Soil and groundwater contamination with gasoline and diesel oil. Assessment of subsurface hydrocarbon contamination resulting from a fuel release from an underground storage tank in Vanstad, Skåne, Sweden.
191. Wennerberg, Hans, 2005: A study of early Holocene climate changes in Småland, Sweden, with focus on the ‘8.2 kyr event’.
192. Nolvi, Maria & Thorelli, Gunilla, 2006: Extraterrestrisk och terrestrisk kromrik spinell i fanerozoiska kondenserade sediment.
193. Nilsson, Andreas, 2006: Palaeomagnetic secular variations in the varved sediments of Lake Goœci¹¿, Poland: testing the stability of the natural remanent magnetization and validity of relative palaeointensity estimates.
194. Nilsson, Anders, 2006: Limnological responses to late Holocene permafrost dynamics at the Stordalen mire, Abisko, northern Sweden.
195. Nilsson, Susanne, 2006: Sedimentary facies and fauna of the Late Silurian Bjärsjölagård Limestone Member (Klinta Formation), Skåne, Sweden.
196. Sköld, Eva, 2006: Kulturlandskapets förändringar inom röjningsröseområdet Yttra Berg, Halland - en pollenanalytisk undersökning av de senaste 5000 åren.
197. Göransson, Ammy, 2006: Lokala miljöförändringar i samband med en plötslig havsyteförändring ca 8200 år före nutid vid Kalvöviken i centrala Blekinge.
198. Brunzell, Anna, 2006: Geofysiska mätningar och visualisering för bedömning av heterogeniteters utbredning i en isälvsavlagring med betydelse för grundvattenflöde.
199. Erlfeldt, Åsa, 2006: Brachiopod faunal dynamics during the Silurian Ireviken Event, Gotland, Sweden.
200. Vollert, Victoria, 2006: Petrografisk och geokemisk karaktärisering av metabasiter i Herrestadsområdet, Småland.
201. Rasmussen, Karin, 2006: En provenansstudie av Kågerödformationen i NV Skåne – tungmineral och petrografi.
202. Karlsson, Jonnina, P., 2006: An investigation of the Felsic Ramiane Pluton, in the Monapo Structure, Northern Moçambique.
203. Jansson, Ida-Maria, 2006: An Early Jurassic conifer-dominated assemblage of the Clarence-Moreton Basin, eastern Australia.
204. Striberger, Johan, 2006: En lito- och biostratigrafisk studie av senglaciala sediment från Skuremåla, Blekinge.
205. Bergelin, Ingemar, 2006: $^{40}Ar/^{39}Ar$ geochronology of basalts in Scania, S Sweden: evidence for two pulses at 191-178 Ma and 110 Ma, and their relation to the breakup of Pangea.
206. Edvarssson, Johannes, 2006: Dendrokronologisk undersökning av tallbestånds etablering, tillväxtdynamik och degenerering orsakat av klimatrelaterade hydrologiska variationer på Viss mosse och Åbuamossen, Skåne, södra Sverige, 7300-3200 cal. BP.
207. Stenfeldt, Fredrik, 2006: Litostratigrafiska studier av en platåformad sand- och grusavlagring i Skuremåla, Blekinge.
208. Dahlenborg, Lars, 2007: A Rock Magnetic Study of the Åkerberg Gold Deposit, Northern Sweden.
209. Olsson, Johan, 2007: Två svekofenniska graniter i Bottniska bassängen; utbredning, U-Pb zirkondatering och test av olika abrasionstekniker.
210. Erlandsson, Maria, 2007: Den geologiska utvecklingen av västra Hamrångesynklinalens suprakrustalbergarter, centrala Sverige.
211. Nilsson, Pernilla, 2007: Kvidingedeltat – bildningsprocesser och arkitektonisk uppbyggnadsmodell av ett glacifluvialt Gilbertdelta.
212. Ellingsgaard, Óluva, 2007: Evaluation of wireline well logs from the borehole Kyrkheddinge-4 by comparsion to measured core data.

213. Åkerman, Jonas, 2007. Borrkärnekartering av en Zn-Ag-Pb-mineralisering vid Stenbrånet, Västerbotten.
214. Kurlovich, Dzmitry, 2007: The Polotsk-Kurzeme and the Småland-Blekinge Deformation Zones of the East European Craton: geomorphology, architecture of the sedimentary cover and the crystalline basement.
215. Mikkelsen, Angelica, 2007: Relationer mellan grundvattenmagasin och geologiska strukturer i samband med tunnelborrning genom Hallandsås, Skåne.
216. Trondman, Anna-Kari, 2007: Stratigraphic studies of a Holocene sequence from Taniente Palet bog, Isla de los Estados, South America.
217. Månsson, Carl-Henrik & Siikanen, Jonas, 2007: Measuring techniques of Induced Polarization regarding data quality with an application on a test-site in Aarhus, Denmark and the tunnel construction at the Hallandsås Horst, Sweden.
218. Ohlsson, Erika, 2007: Classification of stony meteorites from north-west Africa and the Dhofar desert region in Oman.
219. Åkesson, Maria, 2008: Mud volcanoes - a review. (15 hskp)
220. Randsalu, Linda, 2008: Holocene relative sea-level changes in the Tasiusaq area, southern Greenland, with focus on the Ta1 and Ta3 basins. (30 hskp)
221. Fredh, Daniel, 2008: Holocene relative sea-level changes in the Tasiusaq area, southern Greenland, with focus on the Ta4 basin. (30 hskp)
222. Anjar, Johanna, 2008: A sedimentological and stratigraphical study of Weichselian sediments in the Tvärkroken gravel pit, Idre, west-central Sweden. (30 hskp)
223. Stefanowicz, Sissa, 2008: Palyno-stratigraphy and palaeoclimatic analysis of the Lower - Middle Jurassic (Pliensbachian - Bathonian) of the Inner Hebrides, NW Scotland. (15 hskp)
224. Holm, Sanna, 2008: Variations in impactor flux to the Moon and Earth after 3.85 Ga. (15 hskp)
225. Bjärnborg, Karolina, 2008: Internal structures in detrital zircons from Hamrånge: a study of cathodoluminescence and back-scattered electron images. (15 hskp)
226. Noresten, Barbro, 2008: A reconstruction of subglacial processes based on a classification of erosional forms at Ramsvikslandet, SW Sweden. (30 hskp)
227. Mehlqvist, Kristina, 2008: En mellanjurassisk flora från Bagå-formationen, Bornholm. (15 hskp)
228. Lindvall, Hanna, 2008: Kortvariga effekter av tefranedfall i lakustrin och terrestrisk miljö. (15 hskp)
229. Löfroth, Elin, 2008: Are solar activity and cosmic rays important factors behind climate change? (15 hskp)
230. Damberg, Lisa, 2008: Pyrit som källa för spårämnen – kalkstenar från övre och mellersta Danien, Skåne. (15 hskp)
331. Cegrell, Miriam & Mårtensson, Jimmy, 2008: Resistivity and IP measurements at the Bolmen Tunnel and Ådalsbanan, Sweden. (30 hskp)
232. Vang, Ina, 2008: Skarn minerals and geological structures at Kalkheia, Kristiansand, southern Norway. (15 hskp)
233. Arvidsson, Kristina, 2008: Vegetationen i Skandinavien under Eem och Weichsel samt fallstudie i submoräna organiska avlagringar från Nybygget, Småland. (15 hskp)
234. Andersson, Jonas, 2008: An environmental magnetic study of a marine sediment core from Disko Bugt, West Greenland: implications for ocean current variability. (30 hskp)
235. Holm, Sanna, 2008: Titanium- and chromium-rich opaque minerals in condensed sediments: chondritic, lunar and terrestrial origins. (30 hskp)

LUNDS UNIVERSITET

Geologiska institutionen
Gentrum för GeoBiosfärsvetenskap
Sölvegatan 12, 223 62 Lund